Supporting Information

Selective sensing of pyrophosphate in physiological media using zinc(II)dipicolylamino-functionalised peptides

Vincent E. Zwicker, Benjamin M. Long and Katrina A. Jolliffe

School of Chemistry, The University of Sydney, Sydney, NSW 2006, Australia.

E-mail: kate.jolliffe@sydney.edu.au; Fax: +61 2 9351 3329; Tel: +61 2 9351 2297

Contents

1 NMR Spectra of compounds 1–5 and 1·Zn_2–5·Zn_2

Compound 1, ^{1}H NMR (CD_3OD, 500 MHz)

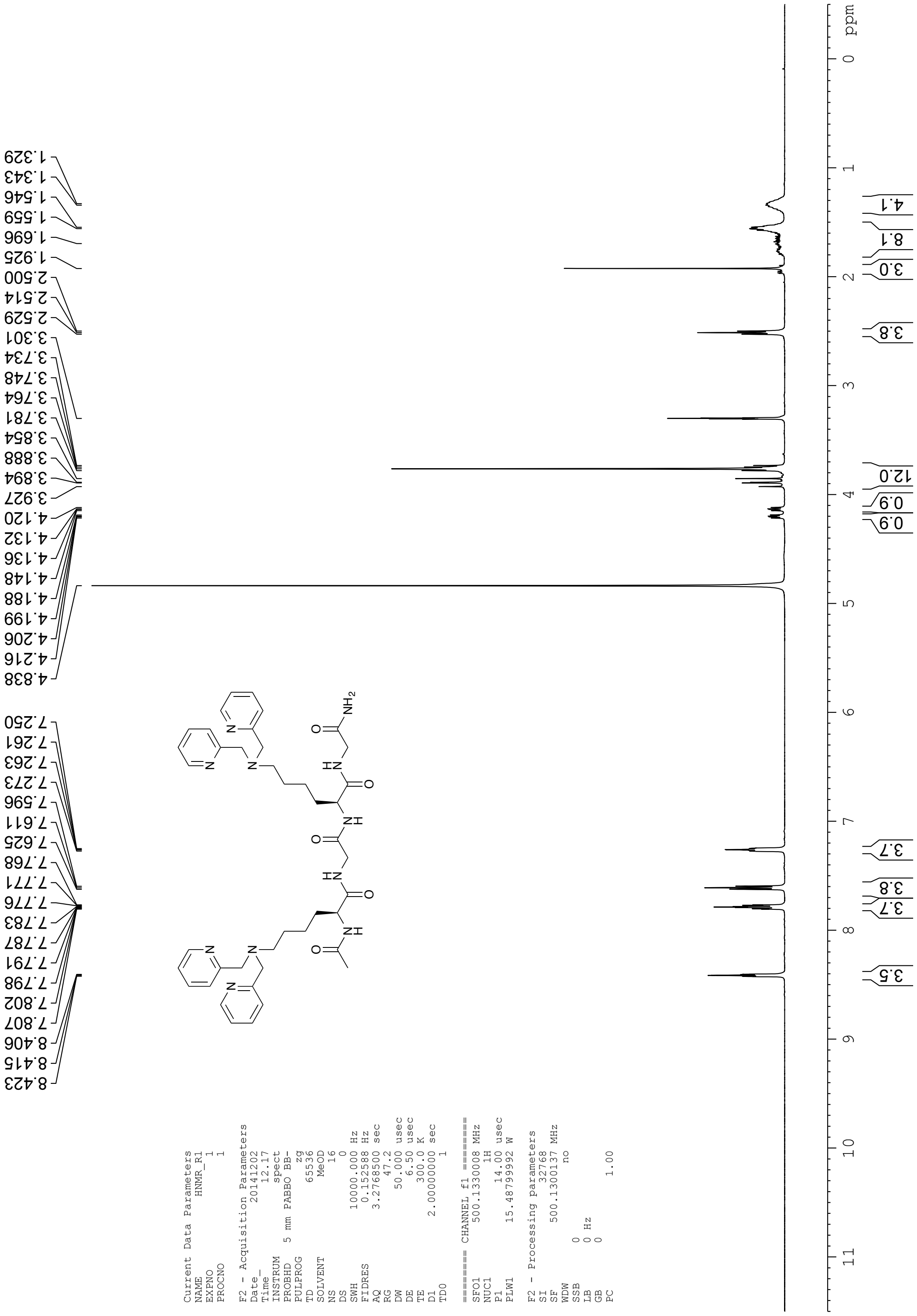

Compound 1, ^{13}C NMR (CD_3OD, 125 MHz)

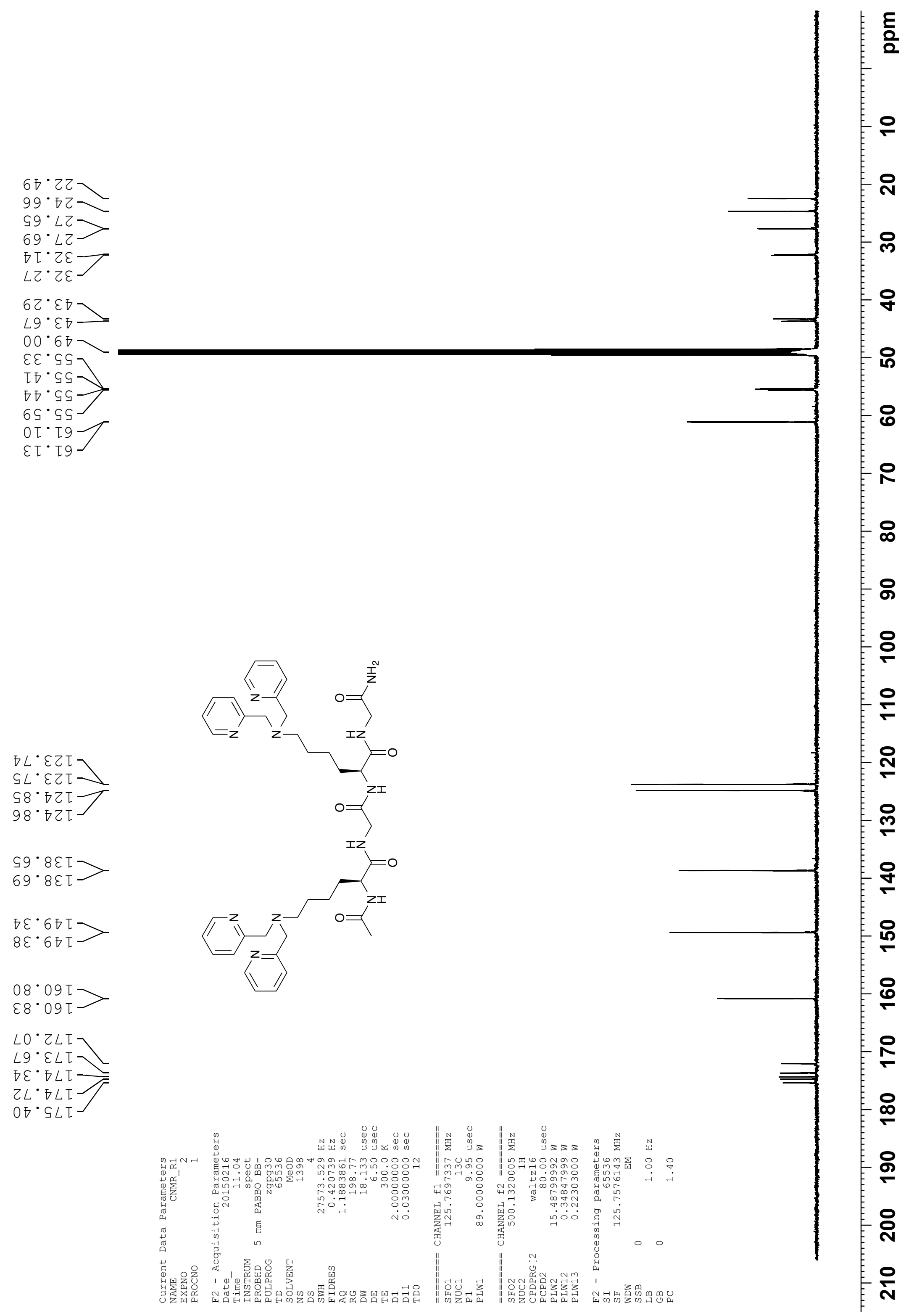

Compound 1·Zn₂, ^{1}H NMR (CD_3OD, 500 MHz)

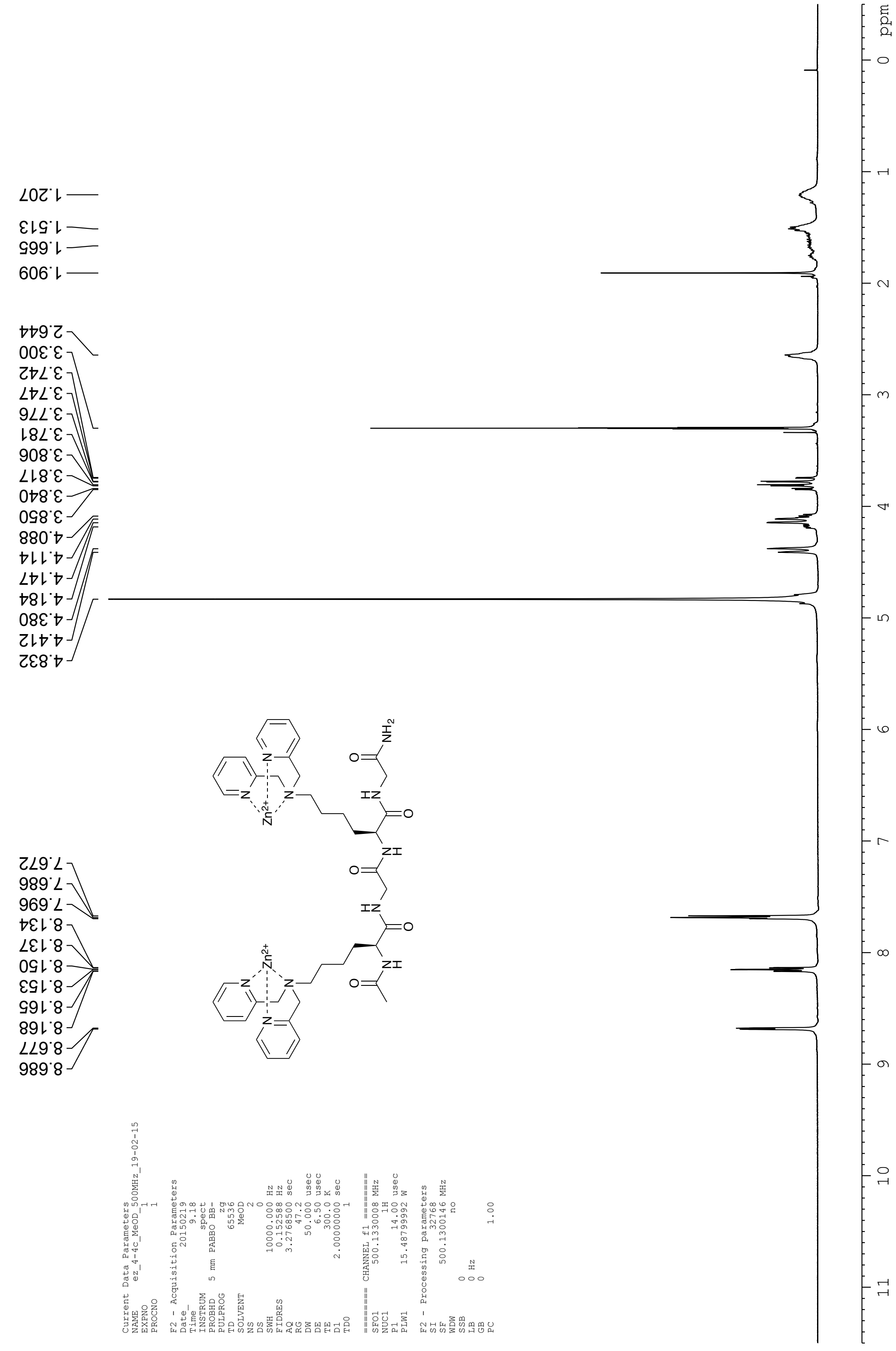

Compound 2, ^{1}H NMR (CD_3OD, 500 MHz)

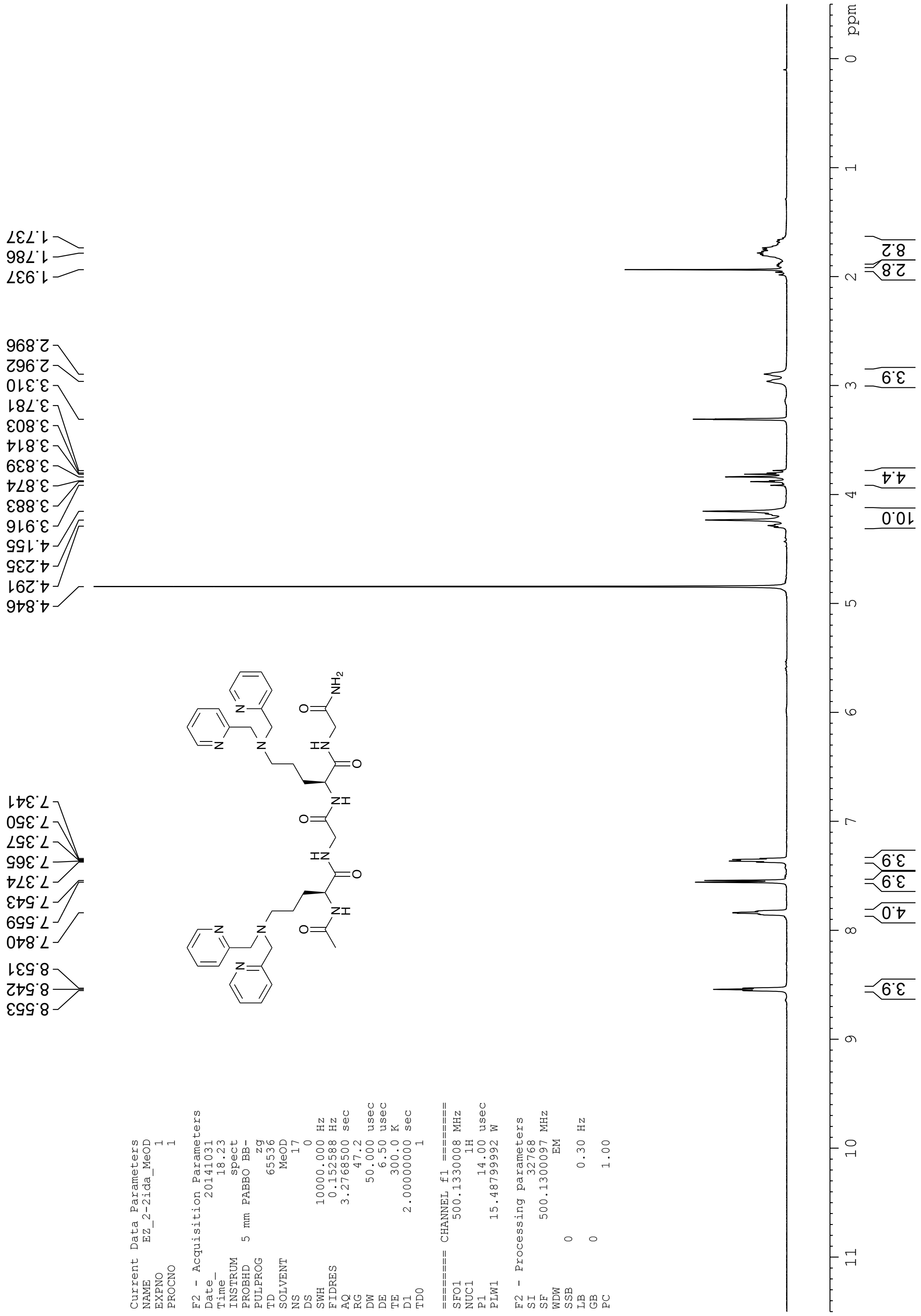

Compound 2, ^{13}C NMR (CD_3OD, 125 MHz)

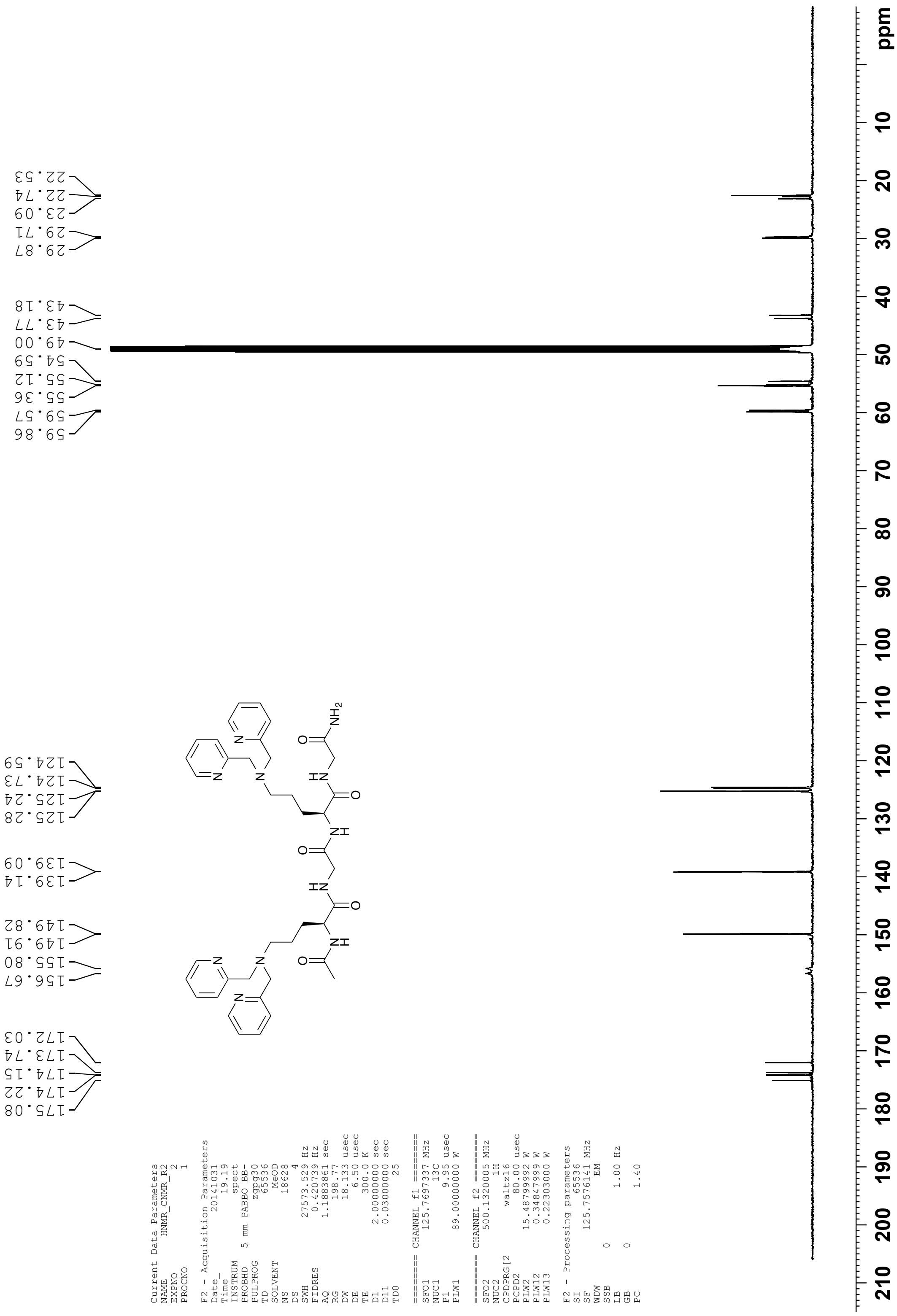

Compound 2·Zn₂, ^{1}H NMR (CD_3OD, 400 MHz)

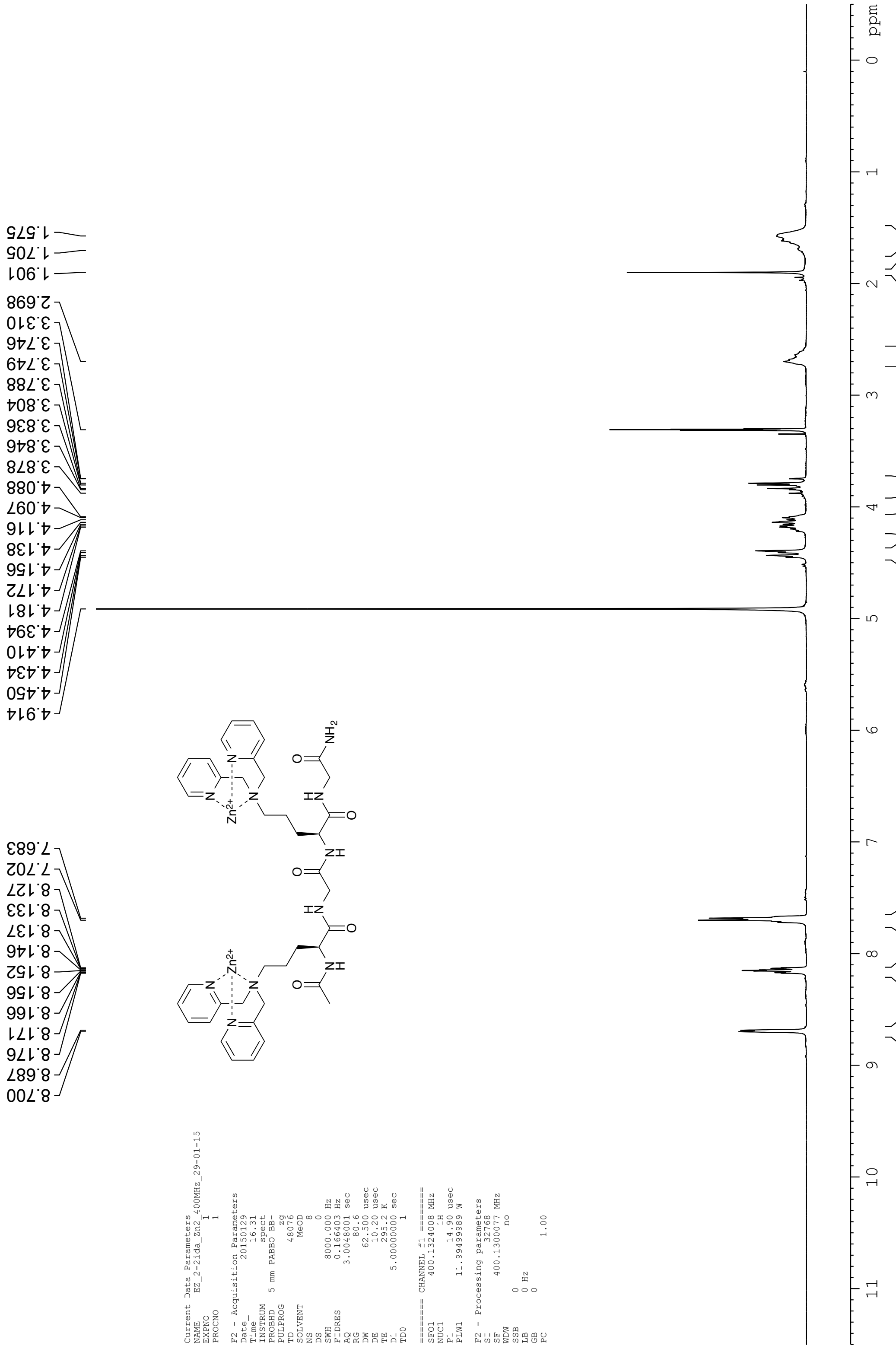

Compound 3, ^{1}H NMR (CD_3OD, 500 MHz)

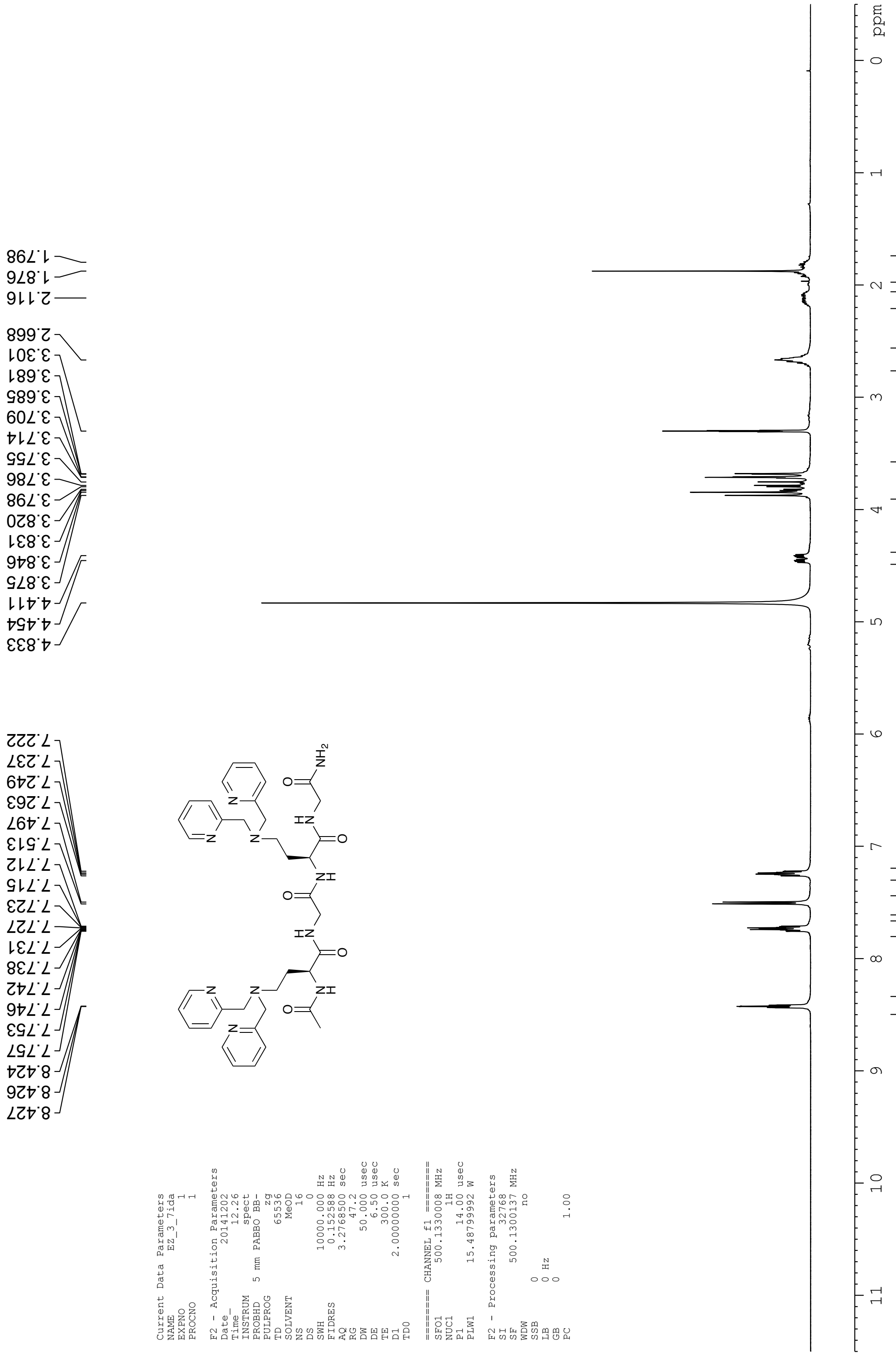

Compound 3, ^{13}C NMR (CD_3OD, 100 MHz)

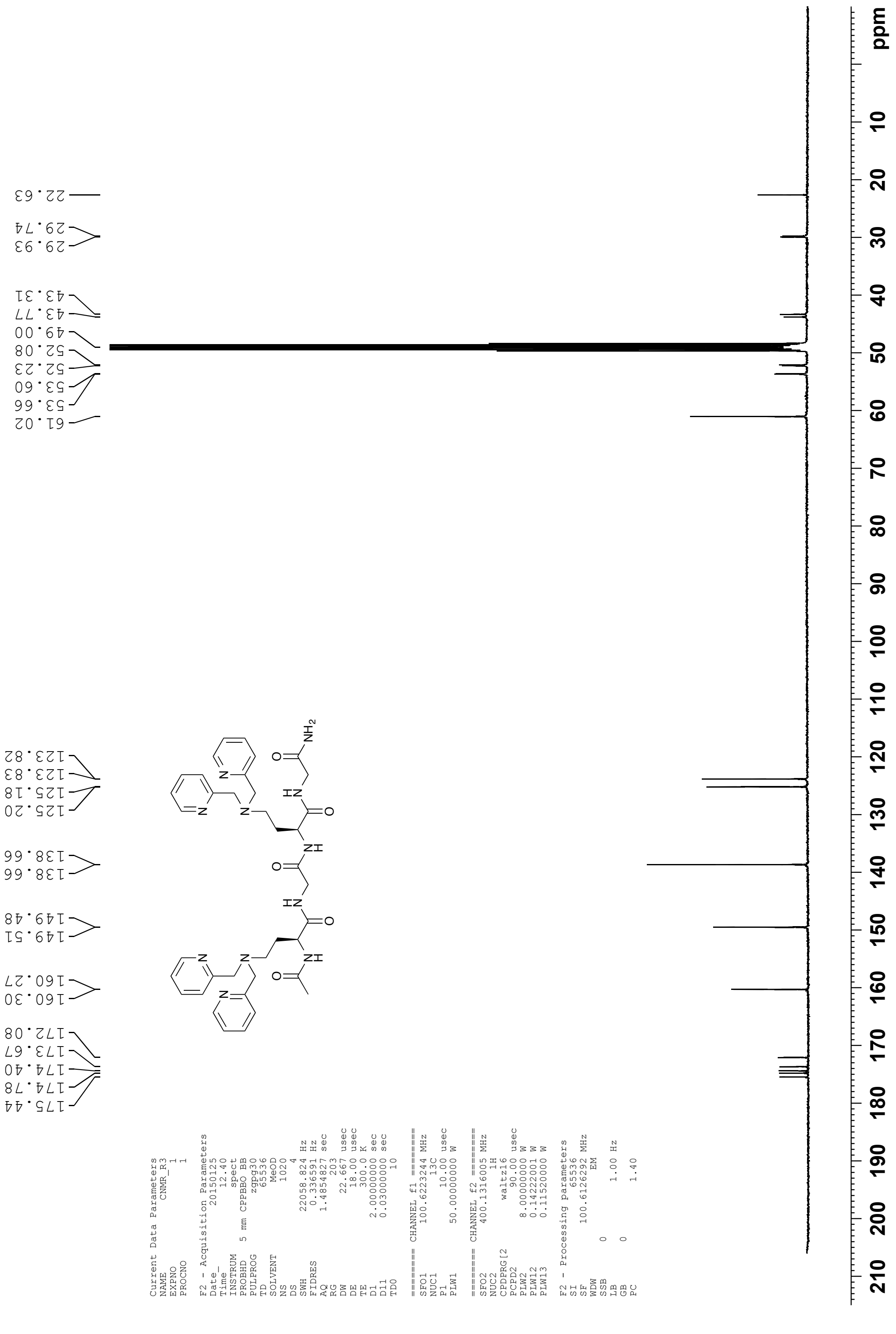

Compound 3·Zn_2, ^{1}H NMR (CD_3OD, 400 MHz)

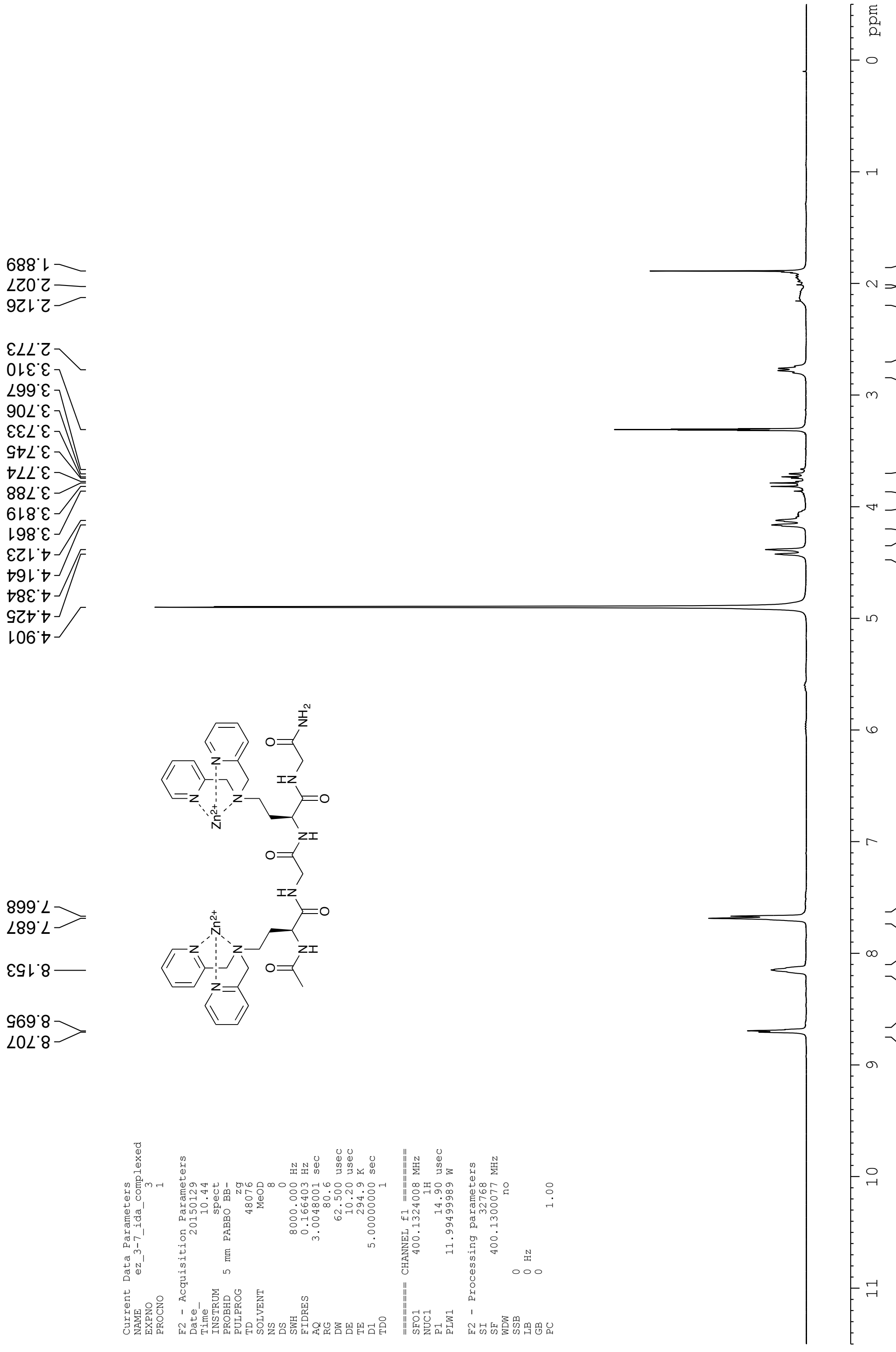

Compound 4, ^{1}H NMR (CD_3OD, 500 MHz)

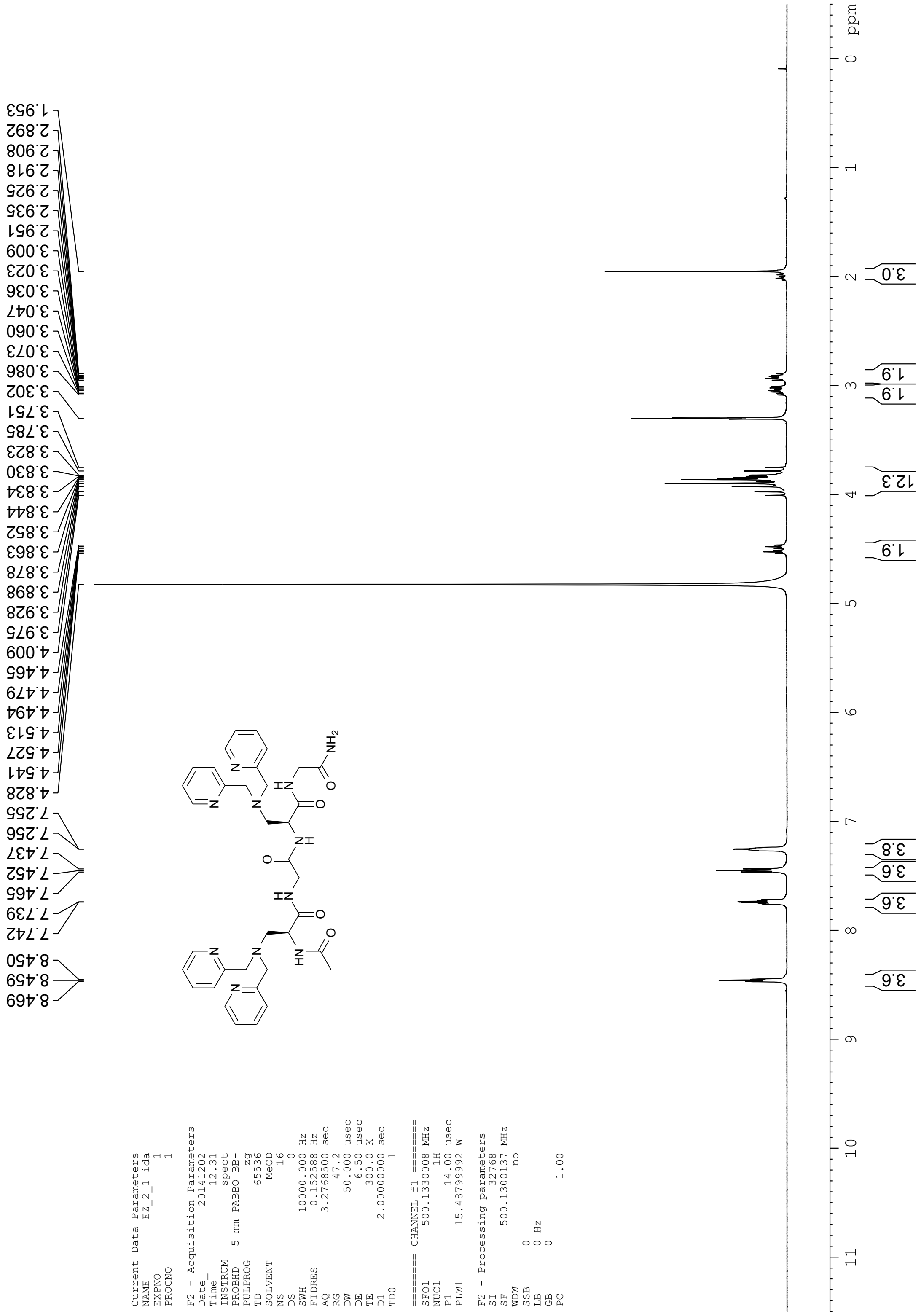

Compound 4, ^{13}C NMR (CD_3OD, 125 MHz)

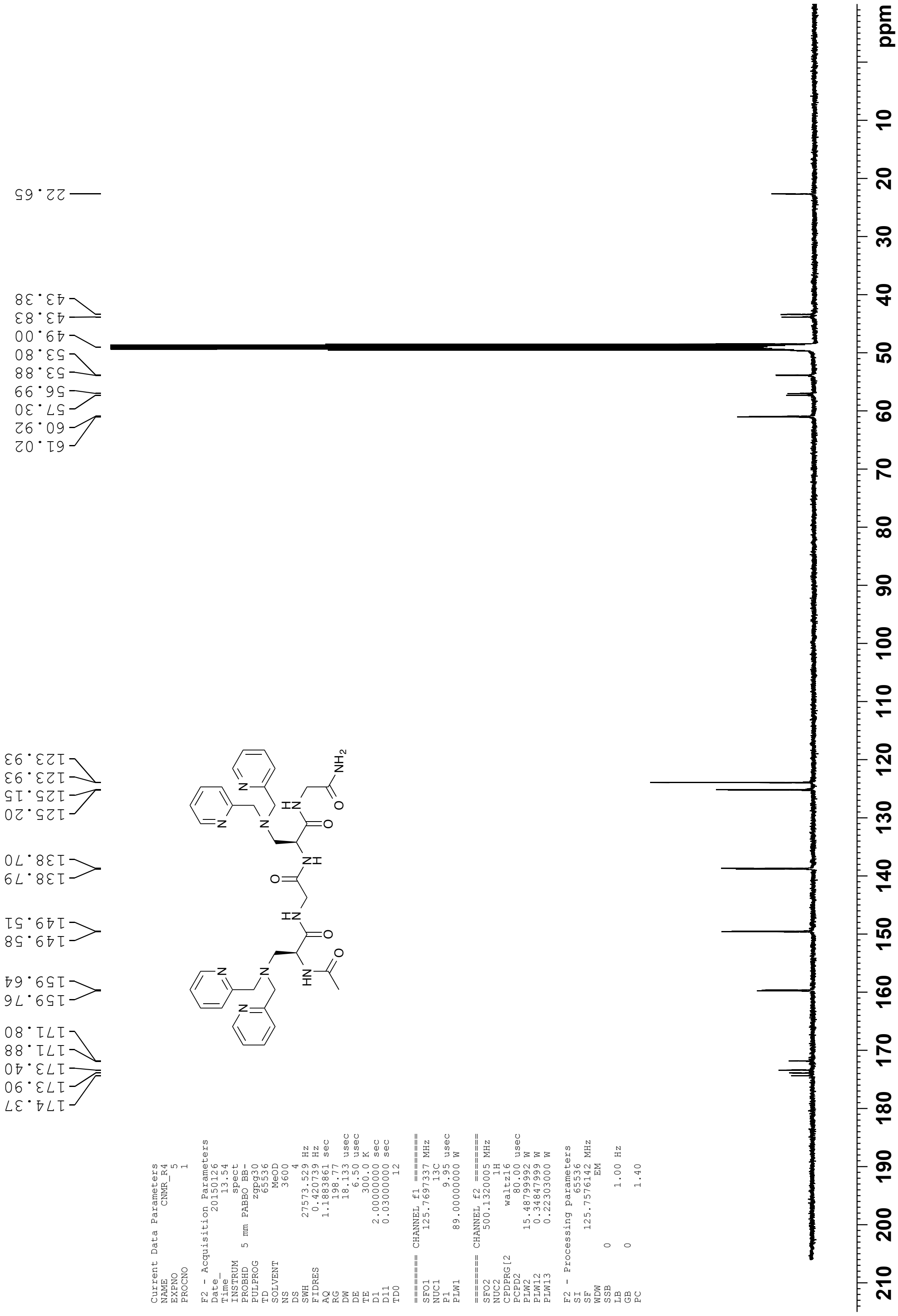

Compound 4·Zn₂, ^{1}H NMR (CD_3OD, 400 MHz)

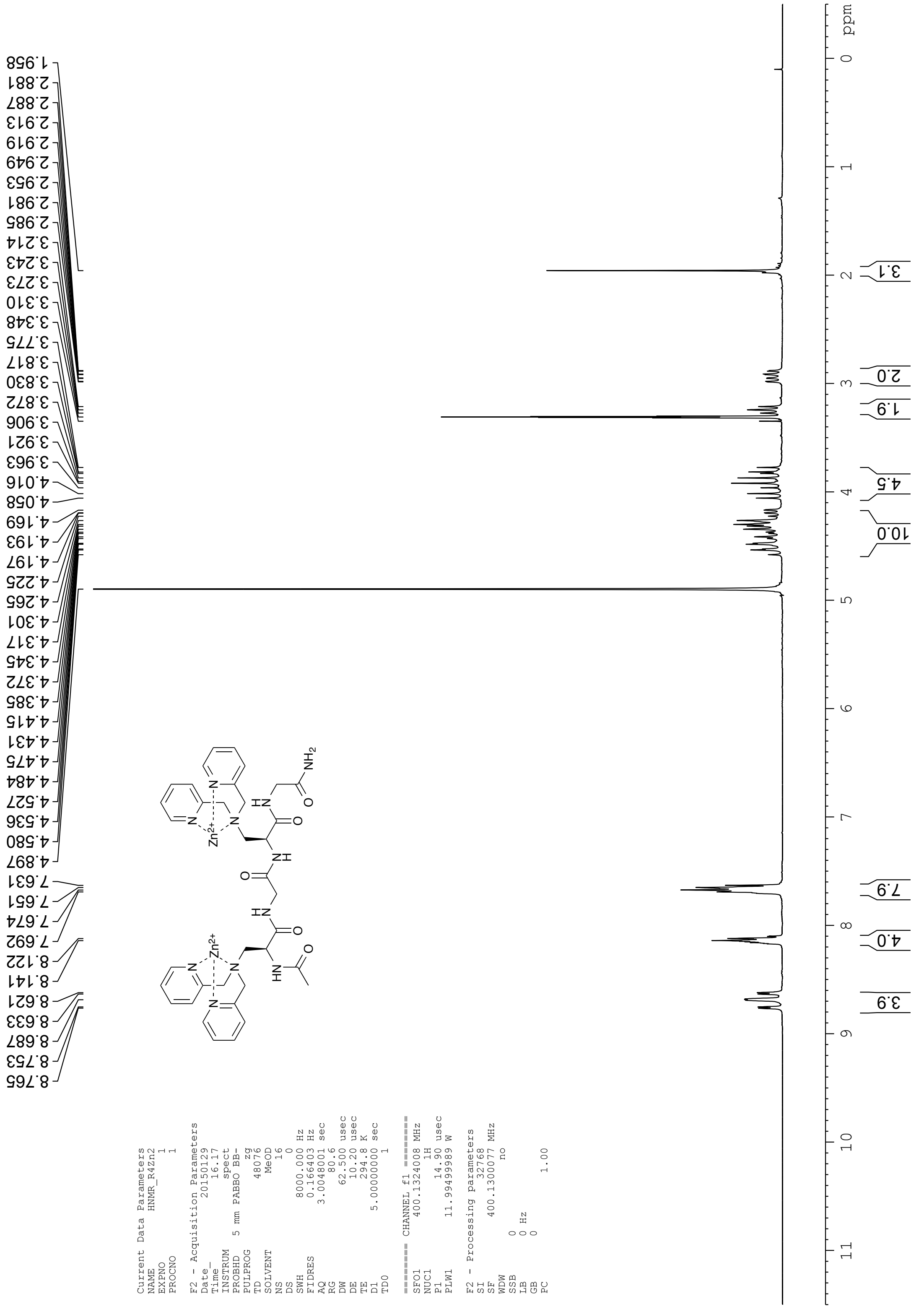

Compound 5, ^{1}H NMR (CD_3OD, 400 MHz)

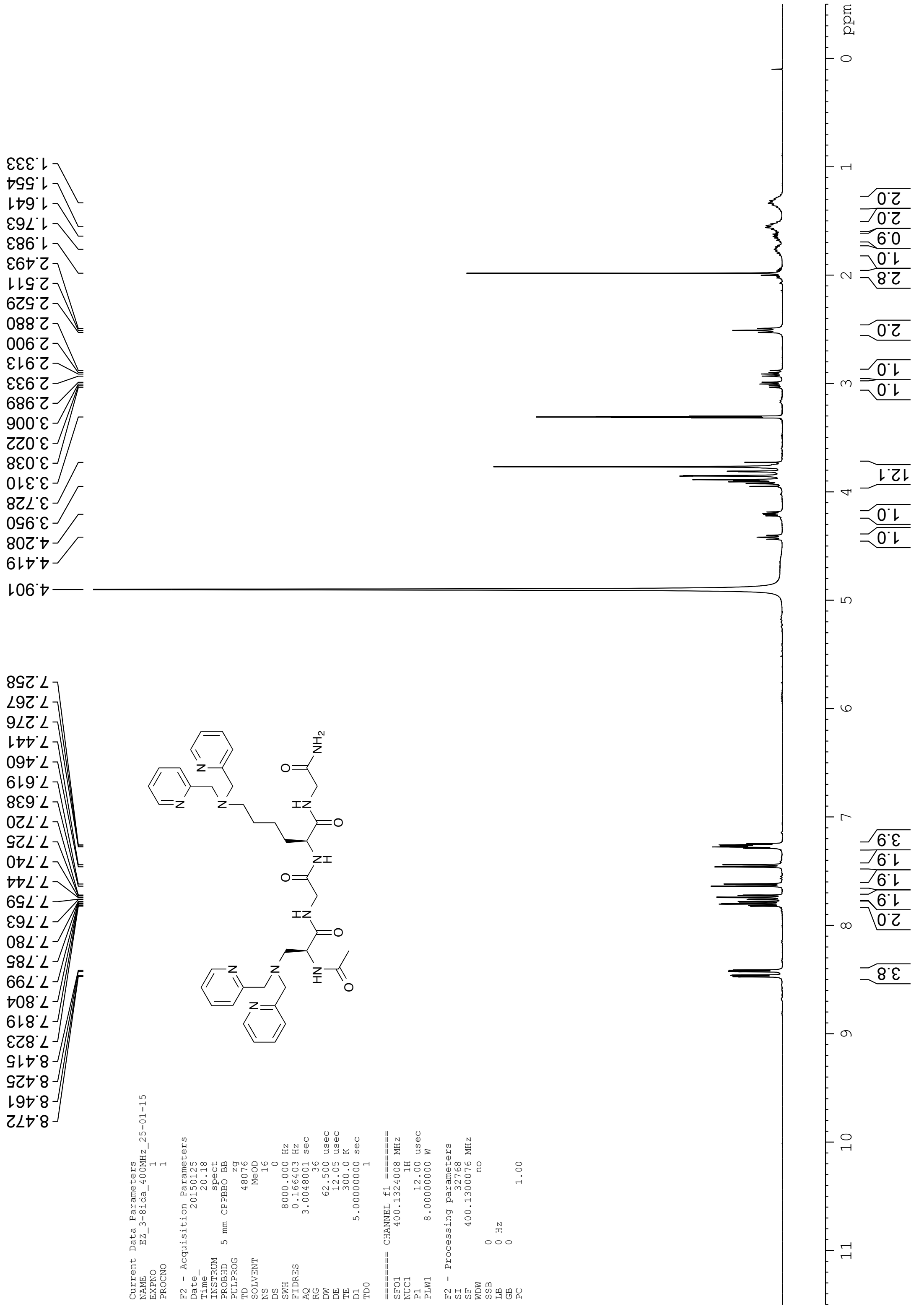

Compound 5, ^{13}C NMR (CD_3OD, 100 MHz)

Compound 5·Zn₂, ^{1}H NMR (CD_3OD, 400 MHz)

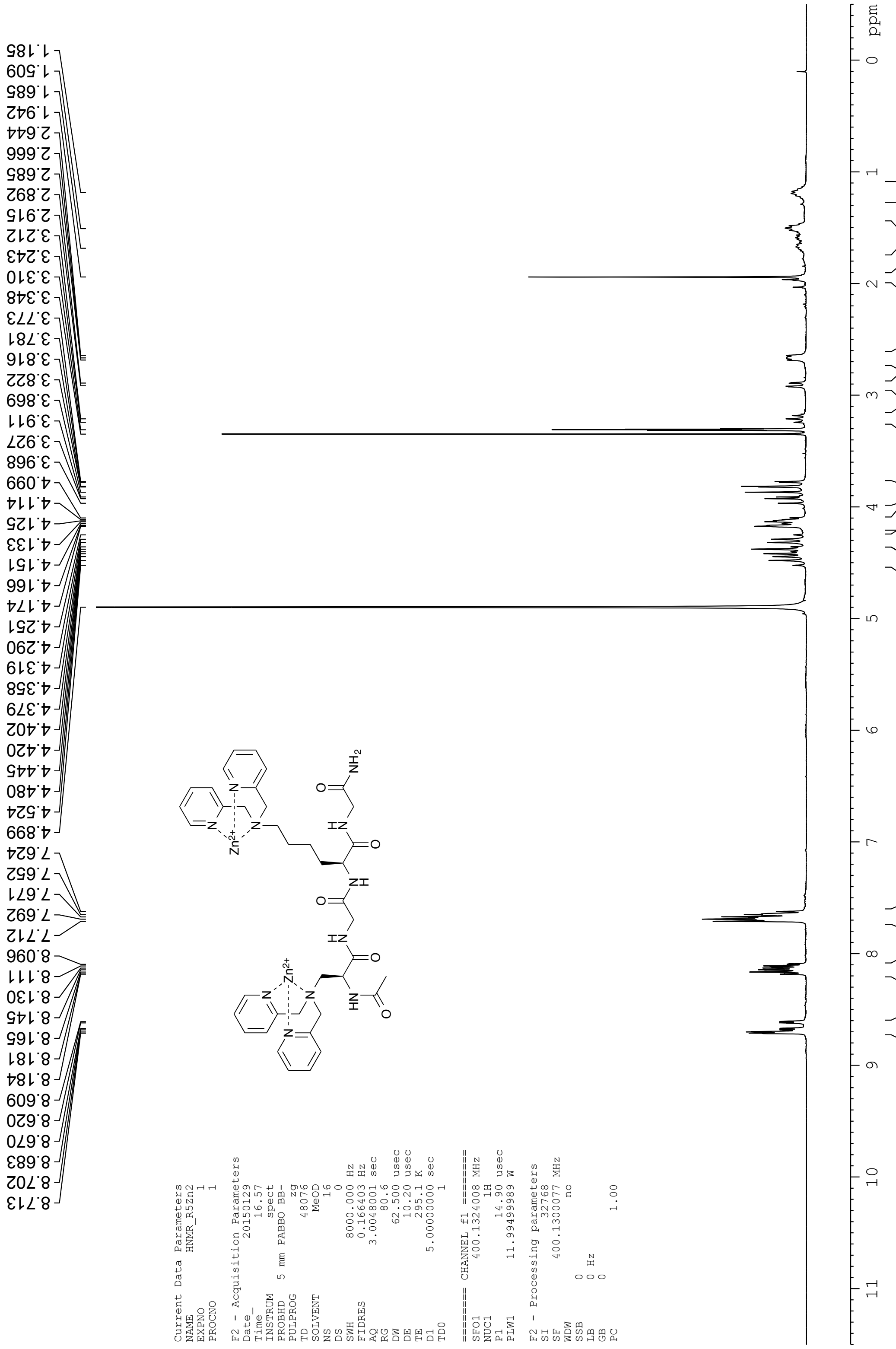

2 Mass spectra of compounds 1–5 and 1·Zn_2–5·Zn_2

Compound 1, High-resolution mass spectrum

Generic Display Report

Analysis Info

Analysis Name	D:\Data\Nick-2014-files\ESI_Positive\10-October\2014-10-30\2014-10-30-posesi-service_000013.d	Acquisition Date	30/10/2014 11:30:25 AM
Method	1MW Positive ESI	Operator	
Sample Name	EZ_2-3	Instrument	apex-Ultra
Comment	CH3OH 1M TOF delay 0.0005s, Q1 200 m/z		

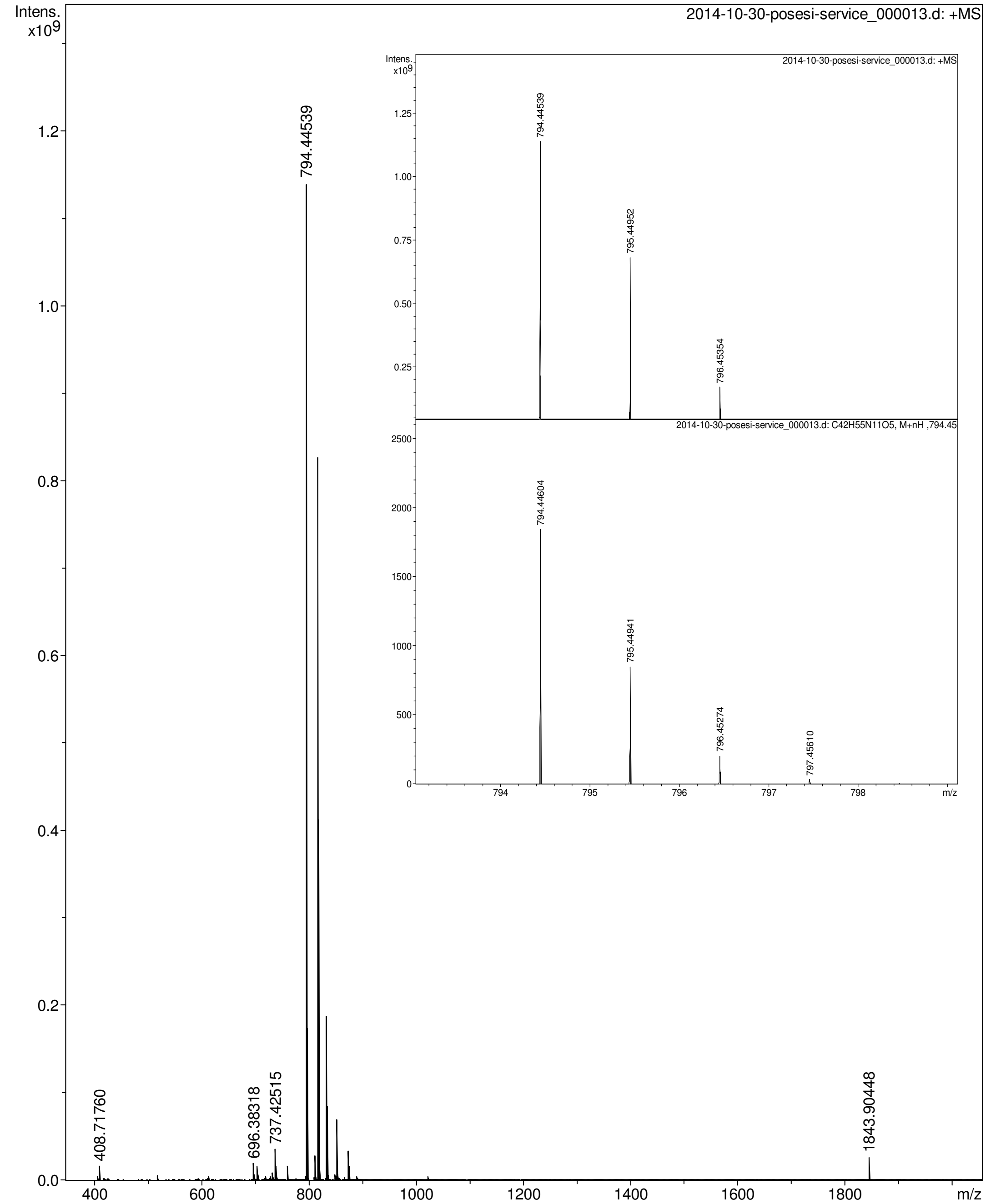

Bruker Compass DataAnalysis 4.0 printed: 30/10/2014 11:33:19 AM Page 1 of 1

Compound 1·Zn_2, High-resolution mass spectrum

Generic Display Report

Analysis Info Acquisition Date 22/01/2015 12:32:40 PM

Analysis Name D:\Data\Nick-2015-files\ESI_Positive\01-January\2015-01-22\2015-01-22-posesi-service_000014.d

Method 1MW Positive ESI Operator

Sample Name EZ_2-3ida_compl Instrument apex-Ultra

Comment MeOH 1M TOF delay 0.0007s, Q1 200 m/z

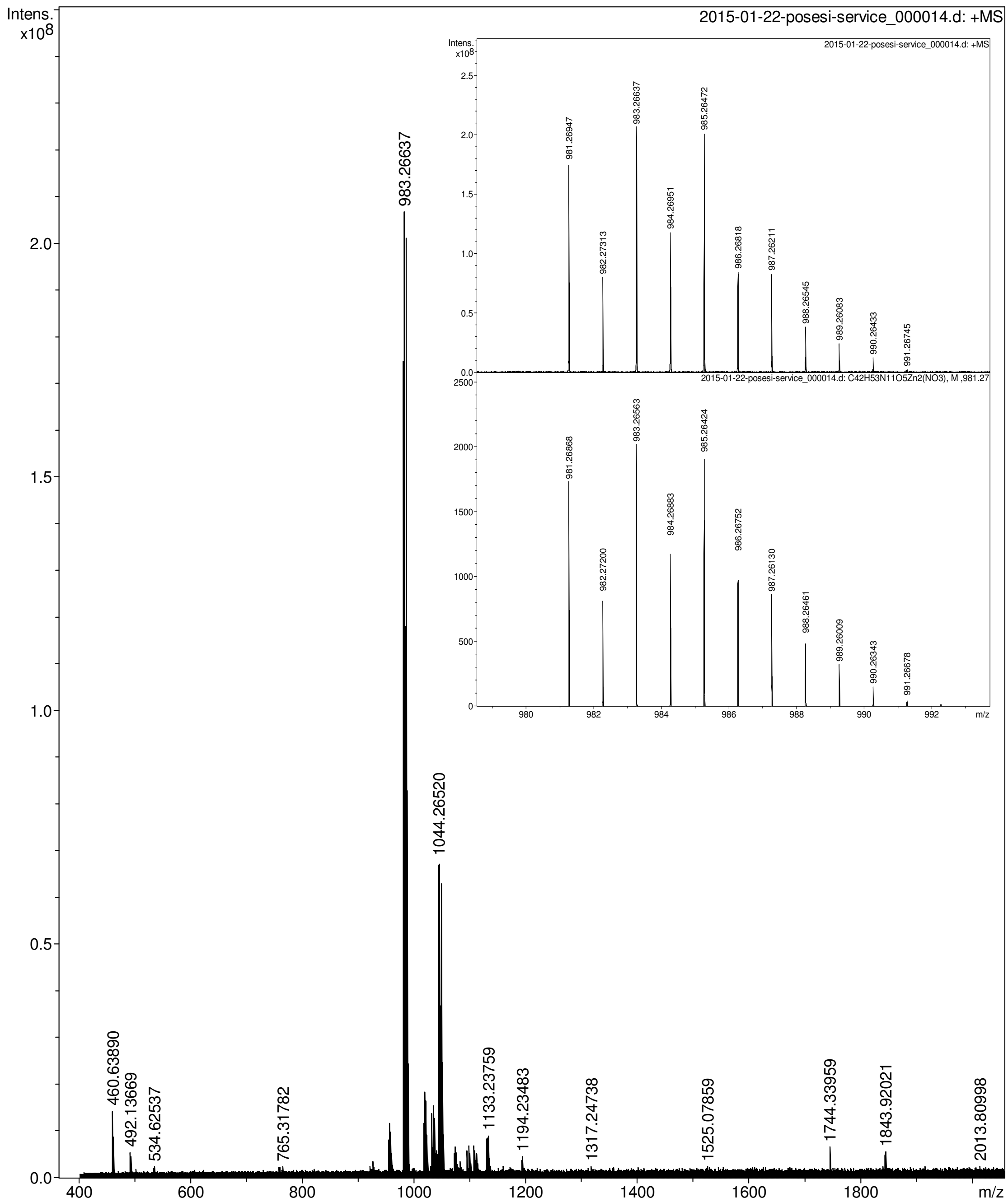

Compound 2, High-resolution mass spectrum

Generic Display Report

Analysis Info		Acquisition Date	20/11/2014 11:01:44 AM
Analysis Name	D:\Data\Nick-2014-files\ESI_Positive\11-November\2014-11-20\2014-11-20-posesi-service_000008.d		
Method	1MW Positive ESI	Operator	
Sample Name	EZ_2-2ida	Instrument	apex-Ultra
Comment	CH3CN 1M TOF delay 0.0005s, Q1 200 m/z		

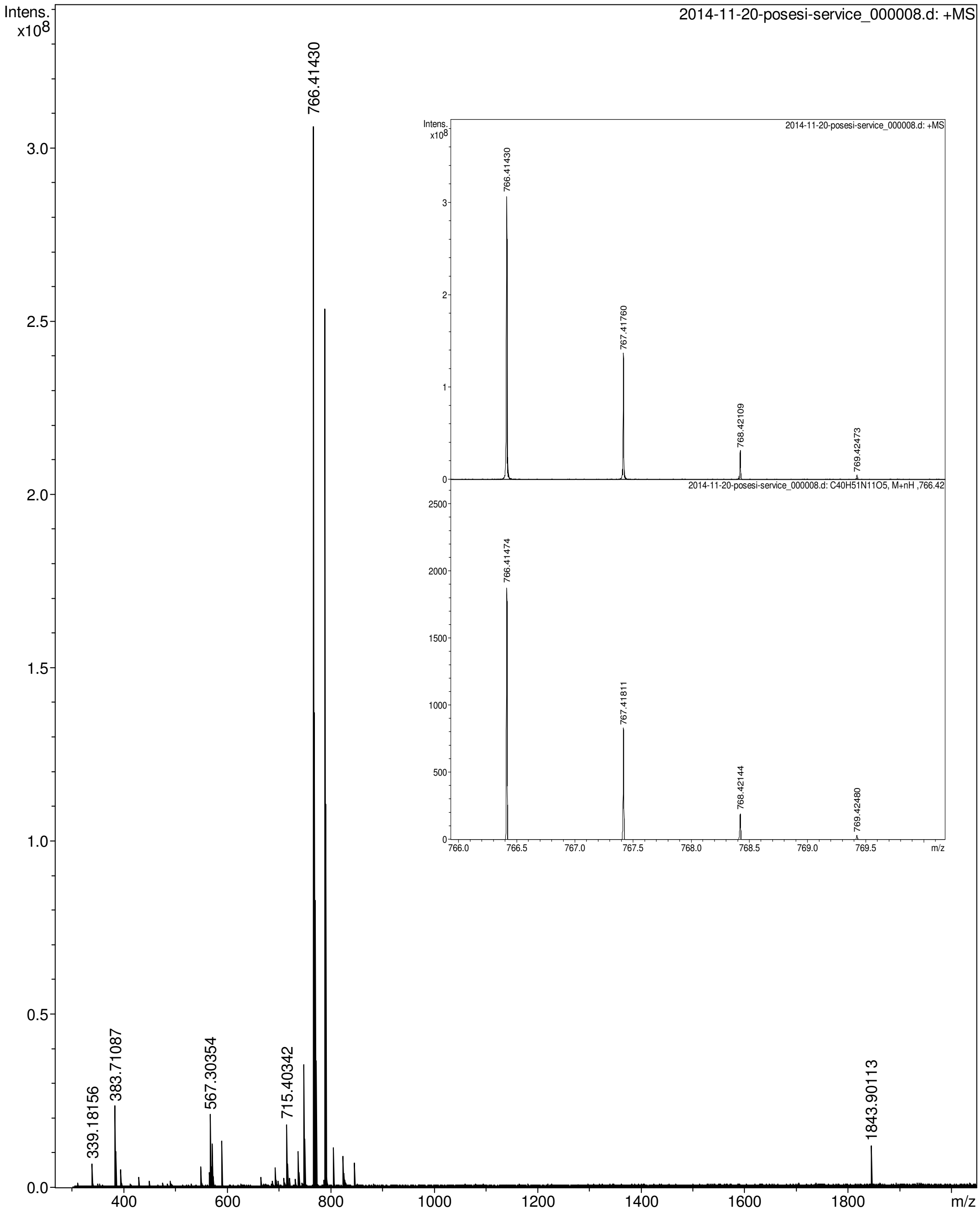

Compound $2{\cdot}Zn_2$, High-resolution mass spectrum

Generic Display Report

Analysis Info		Acquisition Date	22/01/2015 1:55:50 PM
Analysis Name	D:\Data\Nick-2015-files\ESI_Positive\01-January\2015-01-22\2015-01-22-posesi-service_000018.d		
Method	1MW Positive ESI	Operator	
Sample Name	EZ_2-2ida_compl	Instrument	apex-Ultra
Comment	MeOH 1M TOF delay 0.0007s, Q1 200 m/z		

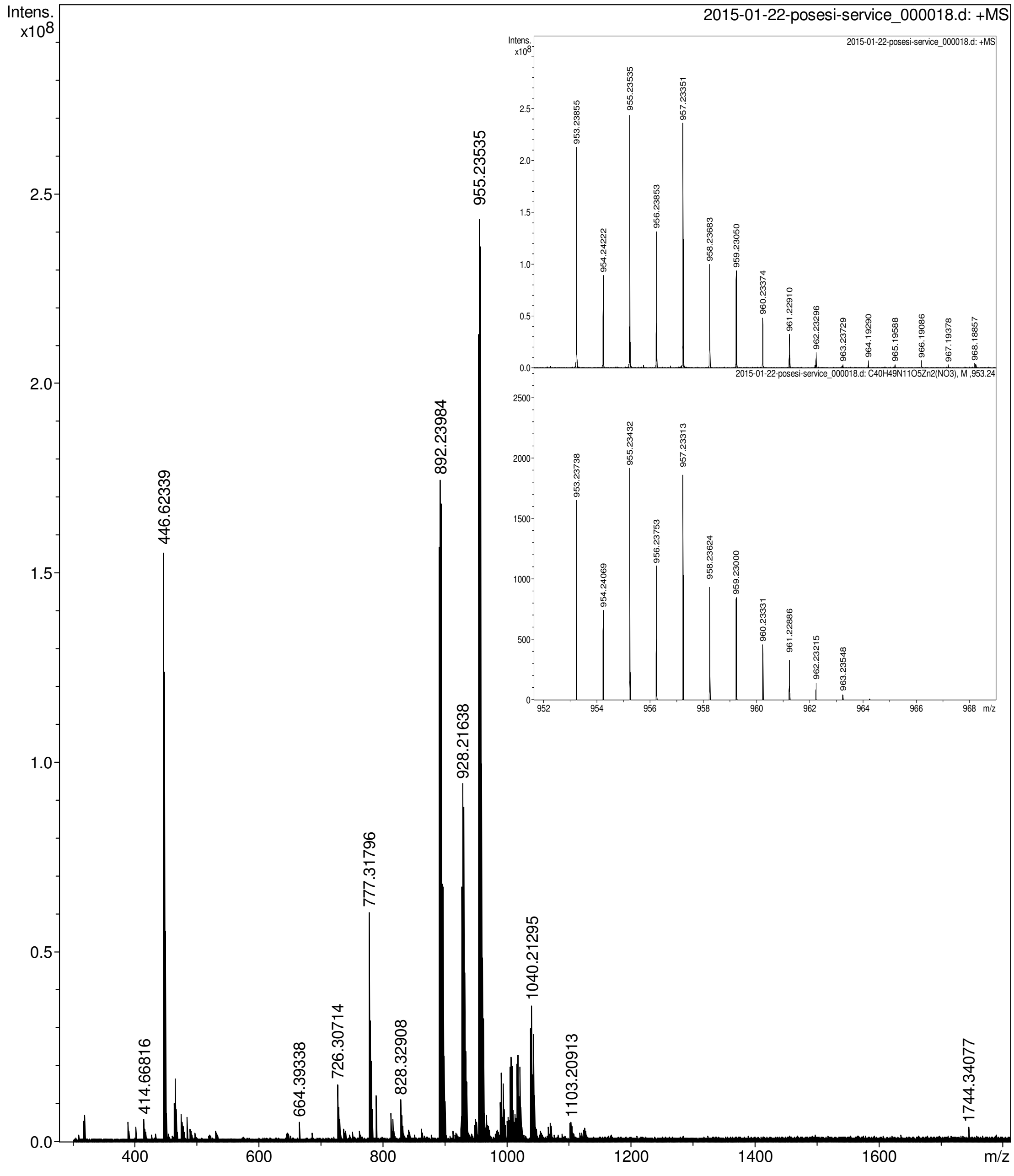

Compound 3, High-resolution mass spectrum

Generic Display Report

Analysis Info		Acquisition Date	
Analysis Name			
Method		Operator	SYSTEM
Sample Name		Instrument	Finnigan-MAT LCQ
Comment			

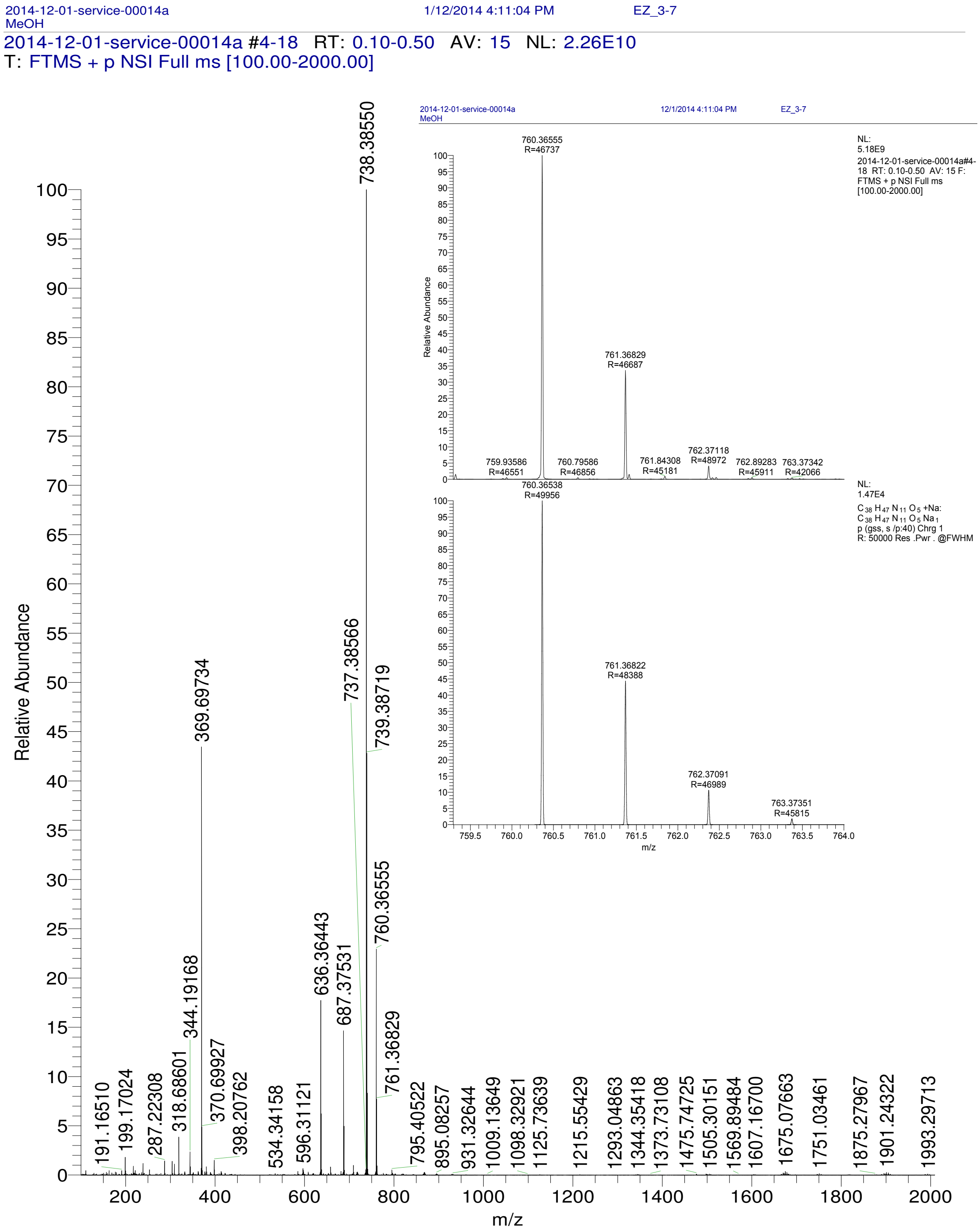

Bruker Daltonics DataAnalysis 3.4 printed: Page 1 of 1

Compound 3·Zn_2, High-resolution mass spectrum

Generic Display Report

Analysis Info		Acquisition Date	22/01/2015 1:00:55 PM
Analysis Name	D:\Data\Nick-2015-files\ESI_Positive\01-January\2015-01-22\2015-01-22-posesi-service_000016.d		
Method	1MW Positive ESI	Operator	
Sample Name	EZ_3-7ida_compl	Instrument	apex-Ultra
Comment	MeOH 1M TOF delay 0.0007s, Q1 200 m/z		

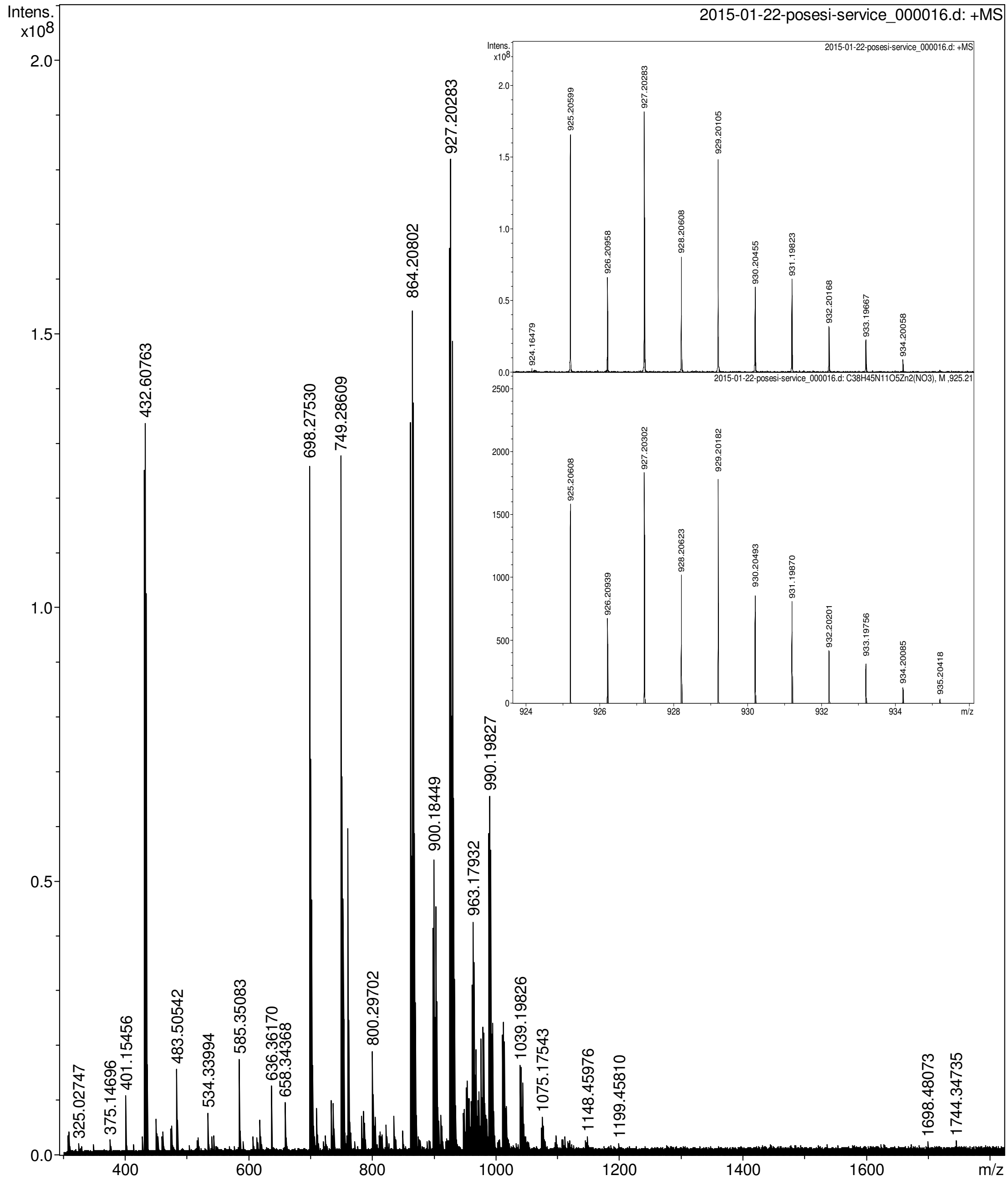

Bruker Compass DataAnalysis 4.0 printed: 22/01/2015 1:11:32 PM Page 1 of 1

Compound 4, High-resolution mass spectrum

Generic Display Report

Analysis Info		Acquisition Date	20/11/2014 10:48:38 AM
Analysis Name	D:\Data\Nick-2014-files\ESI_Positive\11-November\2014-11-20\2014-11-20-posesi-service_000006.d		
Method	1MW Positive ESI	Operator	
Sample Name	EZ_2-1ida	Instrument	apex-Ultra
Comment	CH3CN 1M TOF delay 0.0005s, Q1 200 m/z		

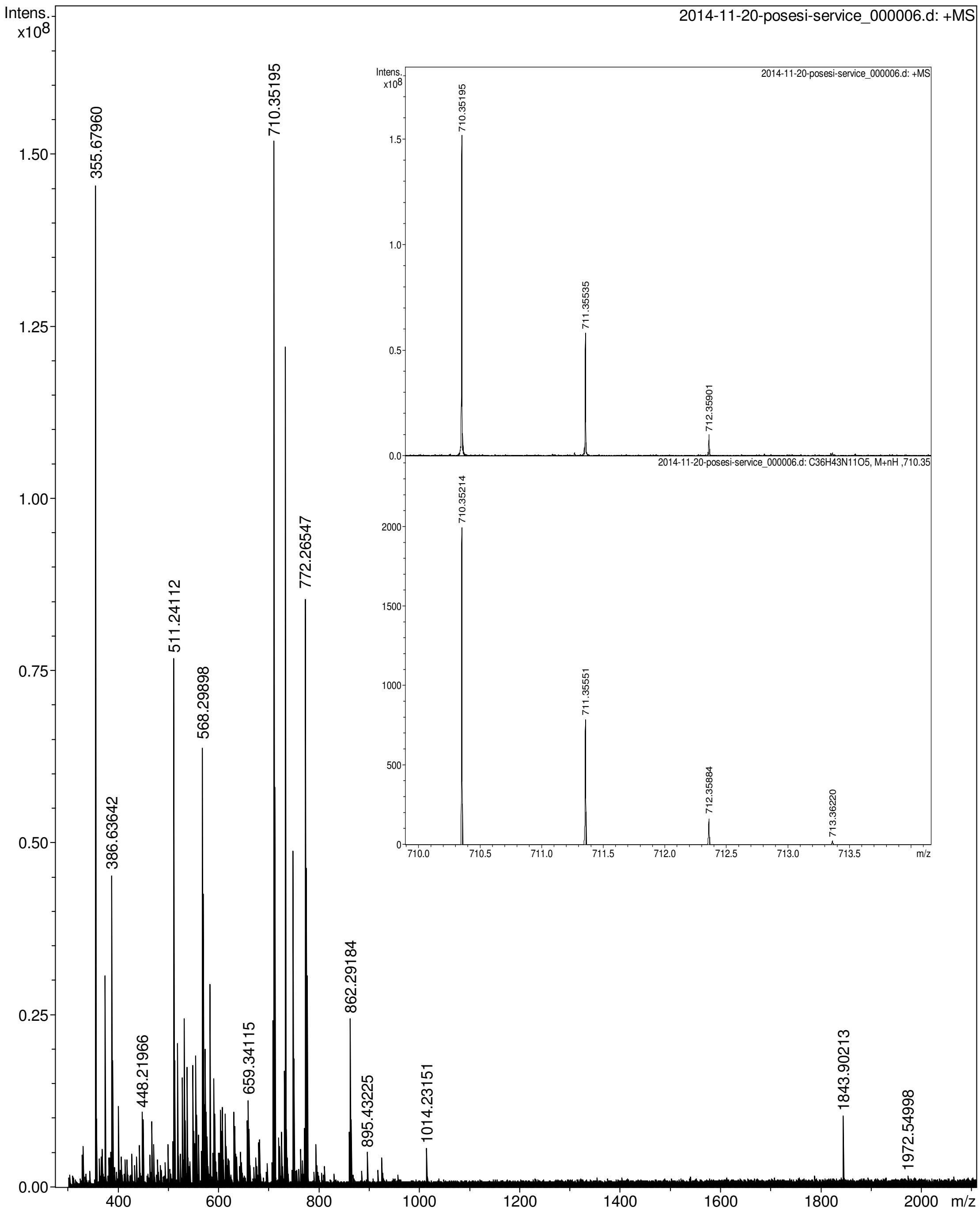

Bruker Compass DataAnalysis 4.0 printed: 20/11/2014 10:52:23 AM Page 1 of 1

Compound 4·Zn_2, High-resolution mass spectrum

Generic Display Report

Analysis Info

Analysis Name	D:\Data\Nick-2015-files\ESI_Positive\01-January\2015-01-22\2015-01-22-posesi-service_000020.d	Acquisition Date	22/01/2015 2:19:39 PM
Method	1MW Positive ESI	Operator	
Sample Name	EZ_2-1ida_compl	Instrument	apex-Ultra
Comment	MeOH 1M TOF delay 0.0007s, Q1 200 m/z		

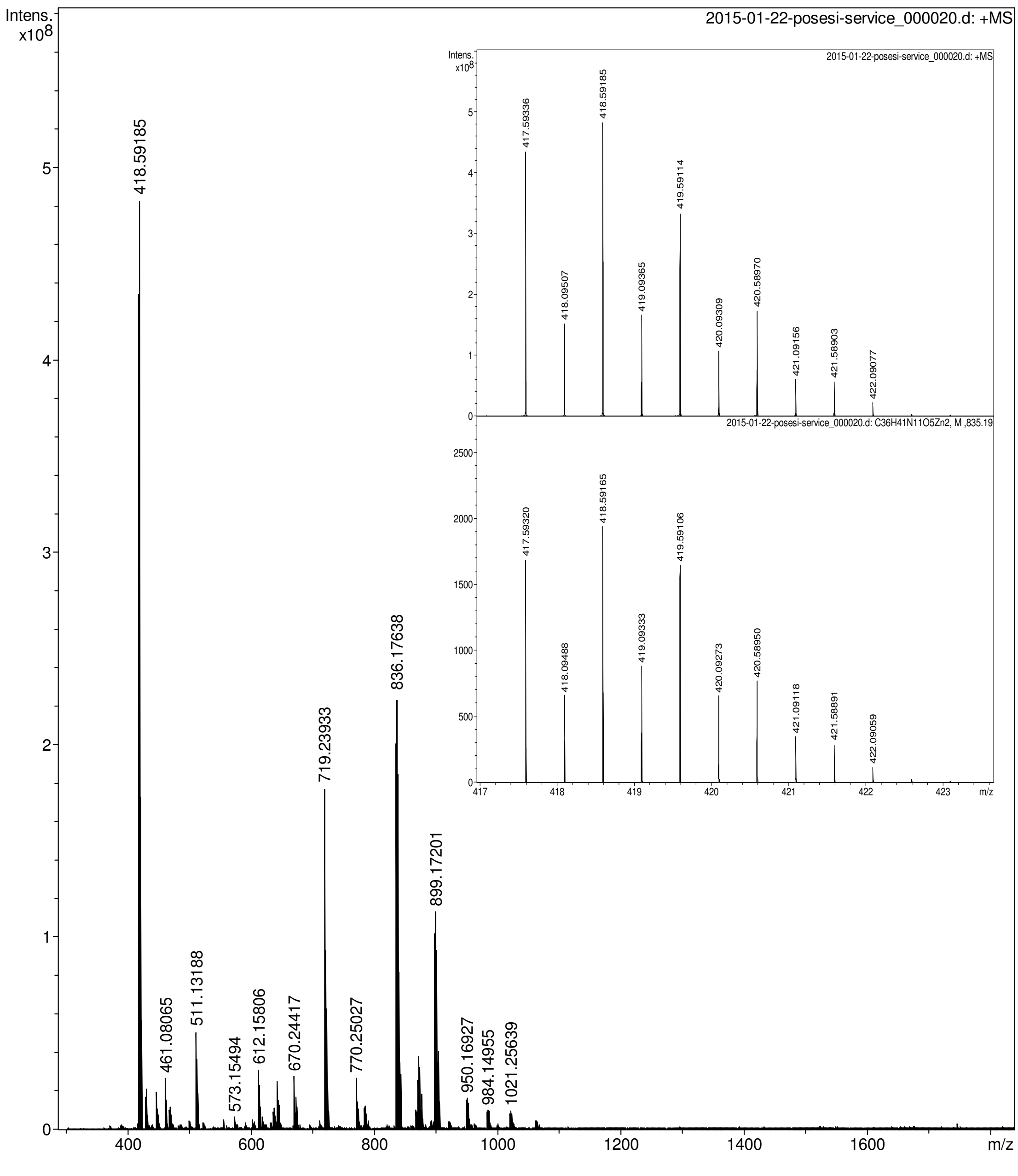

Compound 5, High-resolution mass spectrum

Generic Display Report

Analysis Info		Acquisition Date	1/12/2014 4:04:00 PM
Analysis Name	C:\Xcalibur\data\2014-12-01-service-00013.cdf		
Method		Operator	SYSTEM
Sample Name	EZ_3-8ida	Instrument	Finnigan-MAT LCQ
Comment			

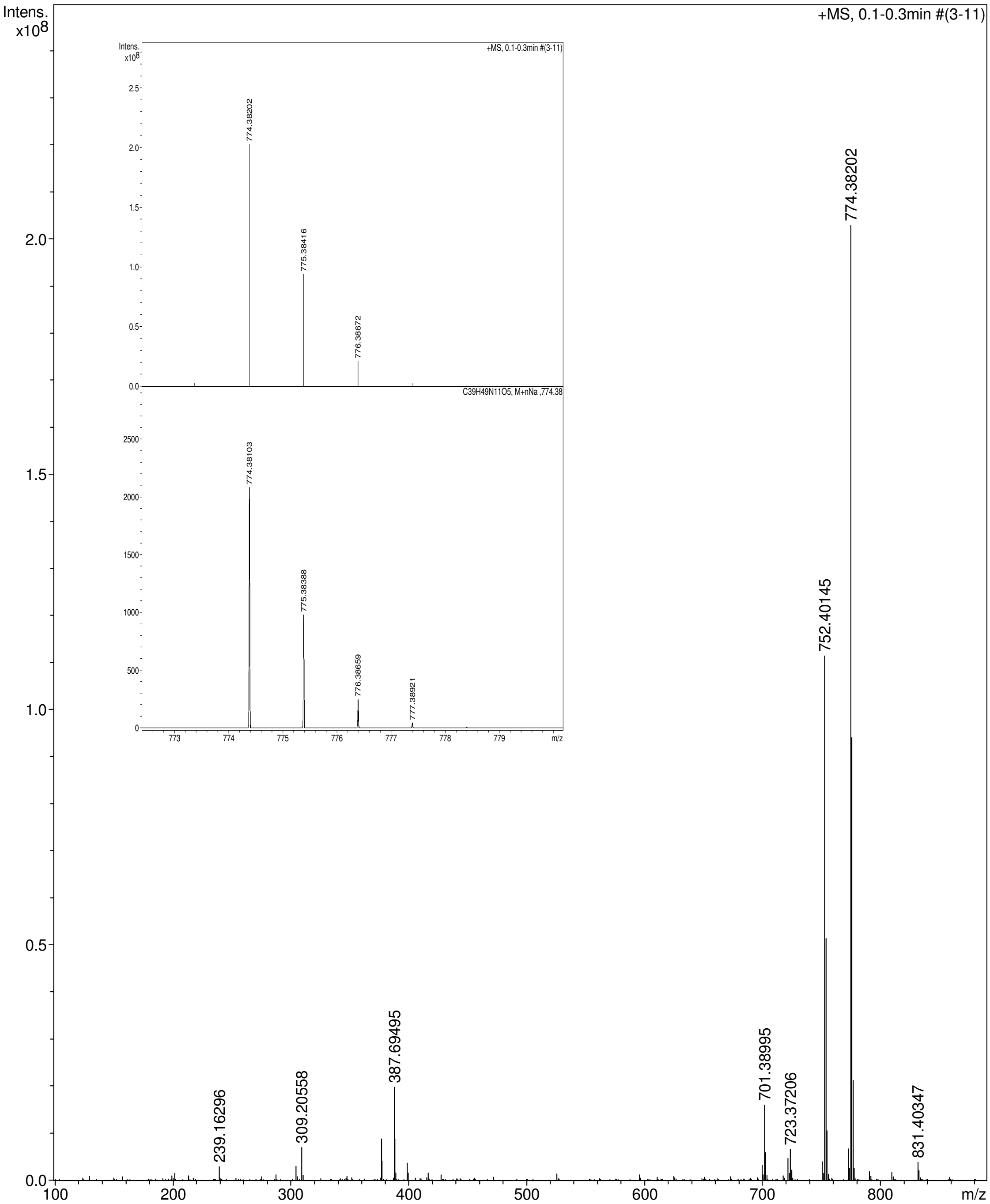

Compound 5·Zn_2, High-resolution mass spectrum

Generic Display Report

Analysis Info | Acquisition Date 22/01/2015 11:49:32 AM

Analysis Name	D:\Data\Nick-2015-files\ESI_Positive\01-January\2015-01-22\2015-01-22-posesi-service_000010.d		
Method	1MW Positive ESI	Operator	
Sample Name	EZ_3-8ida_compl	Instrument	apex-Ultra
Comment	MeOH 1M TOF delay 0.0007s, Q1 200 m/z		

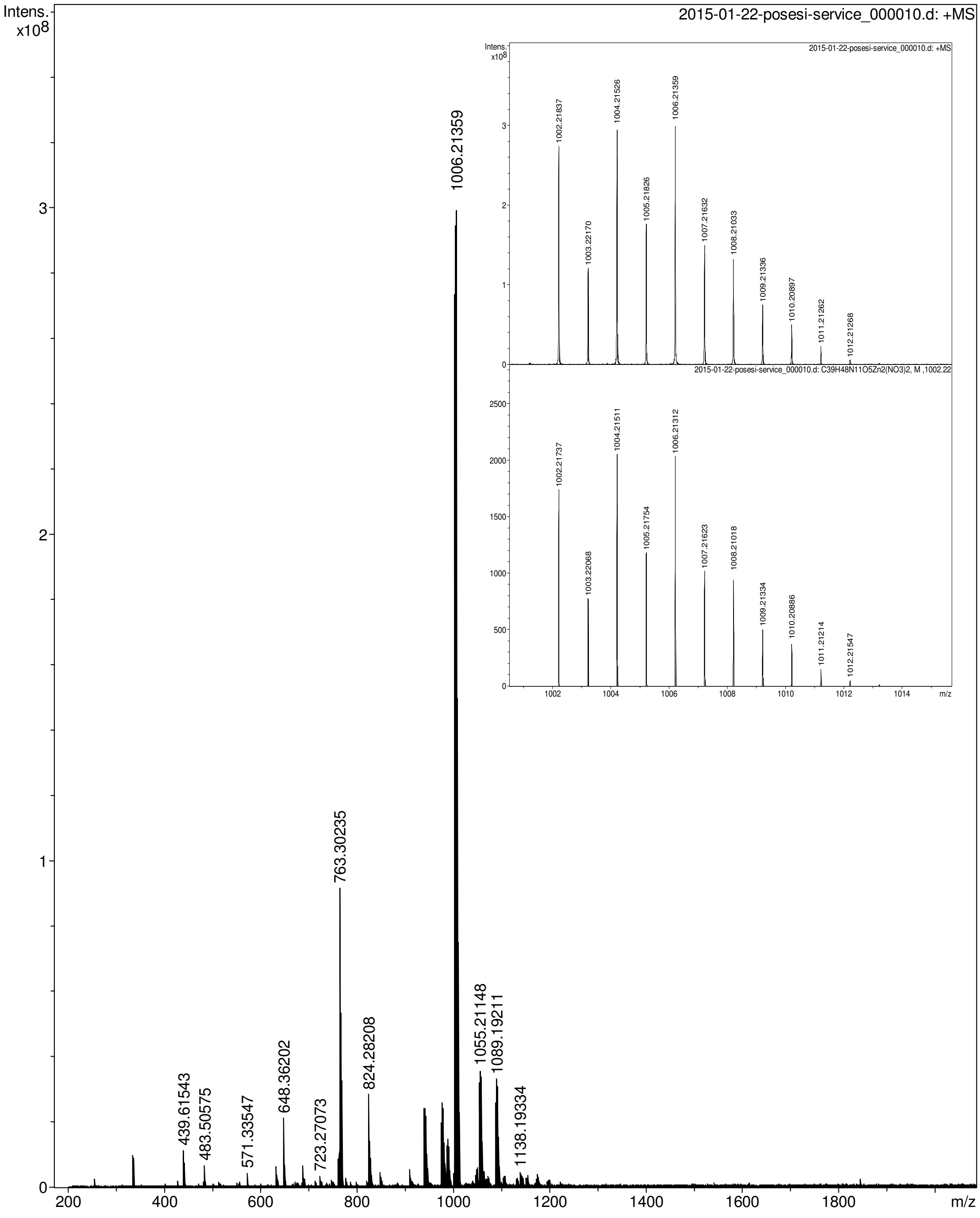

Bruker Compass DataAnalysis 4.0 printed: 22/01/2015 12:08:17 PM Page 1 of 1

3 Anion binding studies conducted in Krebs buffer solution and artificial urine

3.1 Results of the titration of PV solutions with receptors 1–5·Zn_2

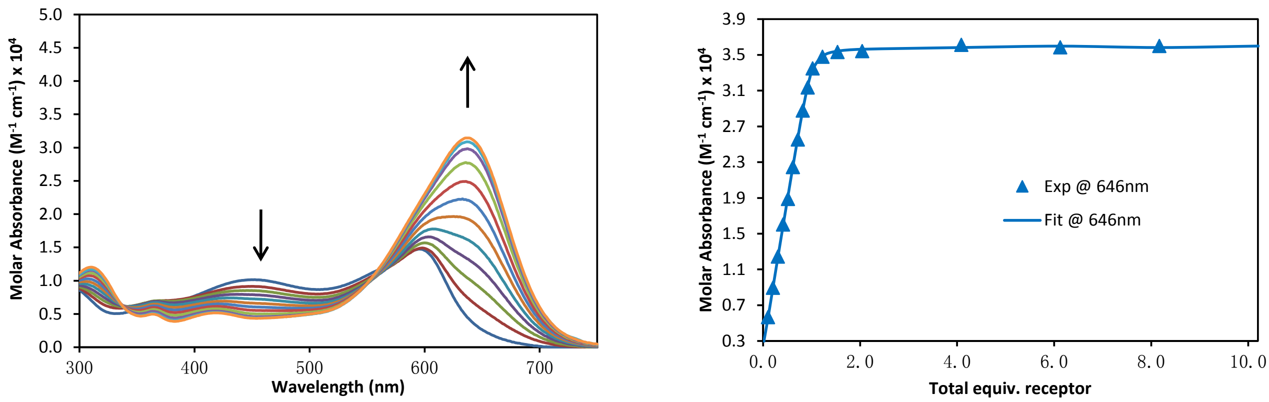

Figure S1: Absorbance changes for **PV** solution (20 µM) in Krebs buffer upon addition of **1·Zn_2** (0 – 10 equiv.). Right: 1 : 1 fitting curve at 646 nm.

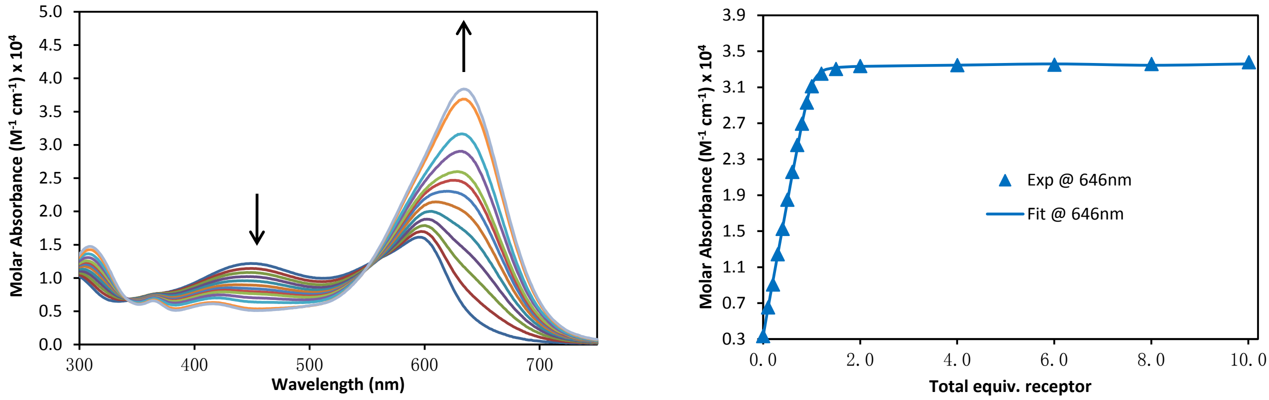

Figure S2: Absorbance changes for **PV** solution (20 µM) in Krebs buffer upon addition of **2·Zn_2** (0 – 10 equiv.). Right: 1 : 1 fitting curve at 646 nm.

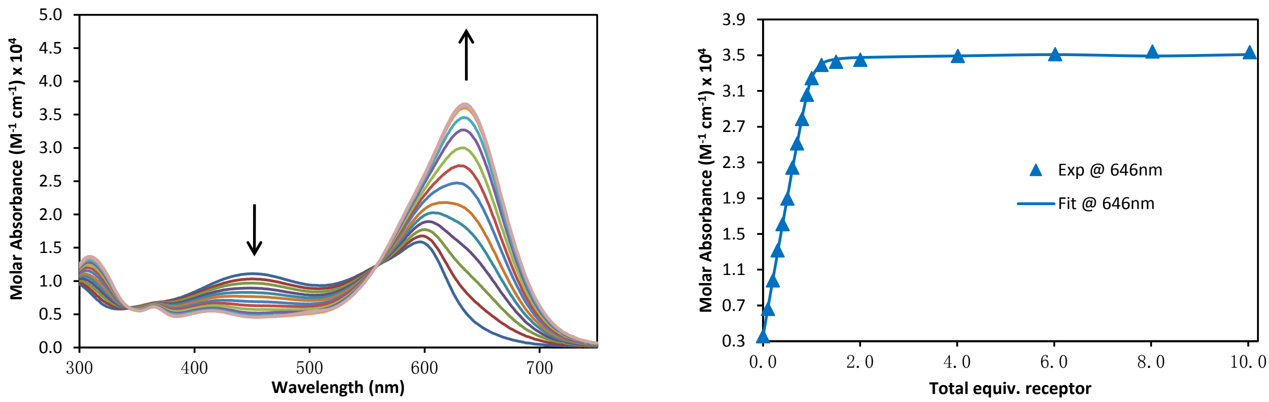

Figure S3: Absorbance changes for **PV** solution (20 µM) in Krebs buffer upon addition of **3·Zn_2** (0 – 10 equiv.). Right: 1 : 1 fitting curve at 646 nm.

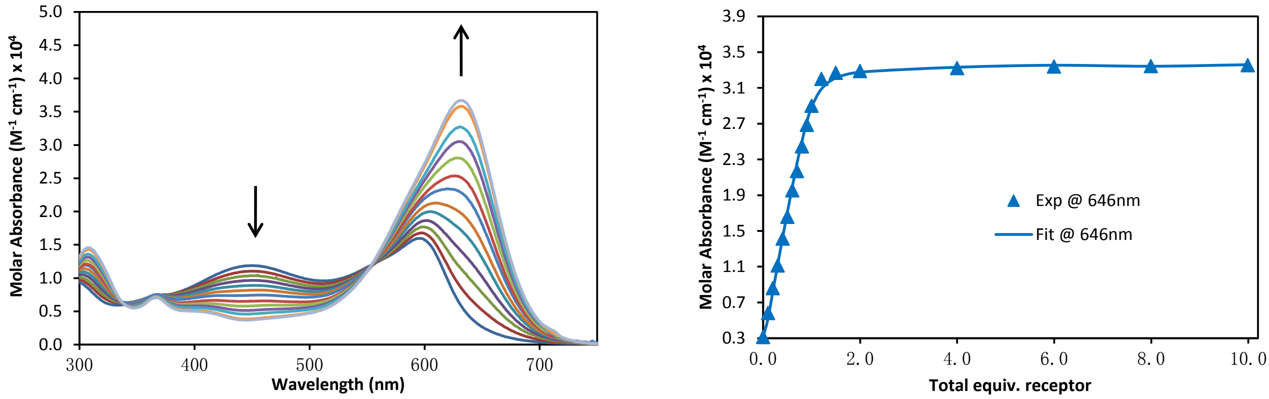

Figure S4: Absorbance changes for **PV** solution (20 μM) in Krebs buffer upon addition of **4·Zn$_2$** (0 – 10 equiv.). Right: 1 : 1 fitting curve at 646 nm.

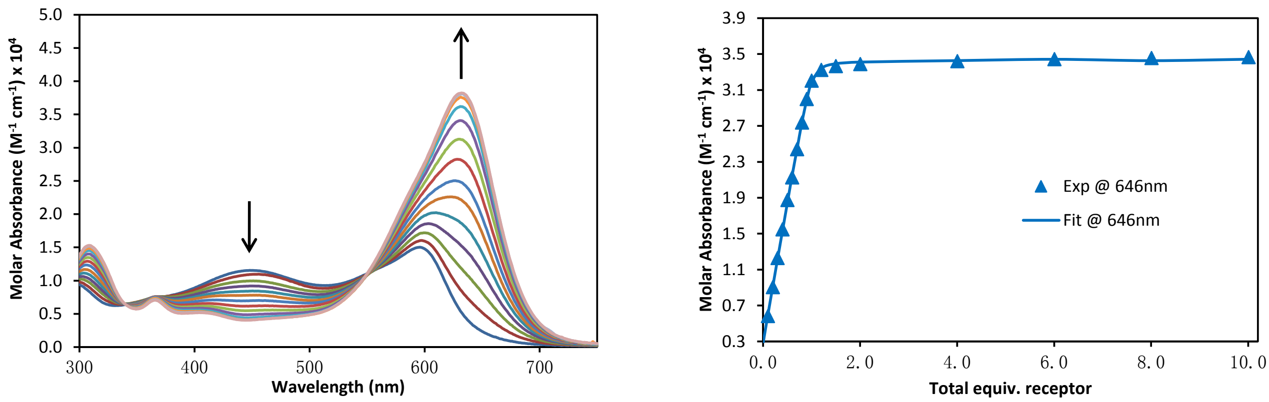

Figure S5: Absorbance changes for **PV** solution (20 μM) in Krebs buffer upon addition of **5·Zn$_2$** (0 – 10 equiv.). Right: 1 : 1 fitting curve at 646 nm.

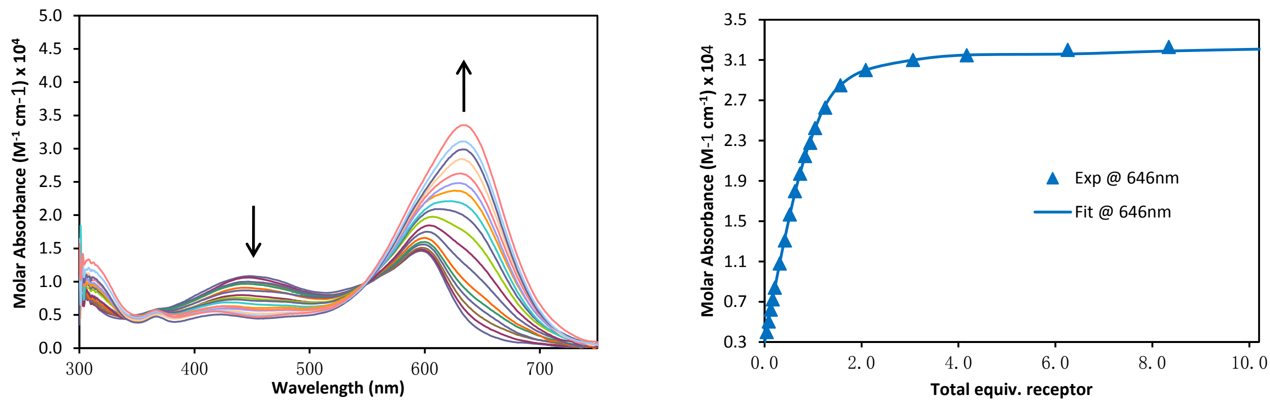

Figure S6: Absorbance changes for **PV** solution (20 μM) in artificial urine upon addition of **3·Zn$_2$** (0 – 10 equiv.). Right: 1 : 1 fitting curve at 646 nm.

3.2 Results of the titration of 1:1–receptor:PV mixtures with PPi, ATP, and ADP

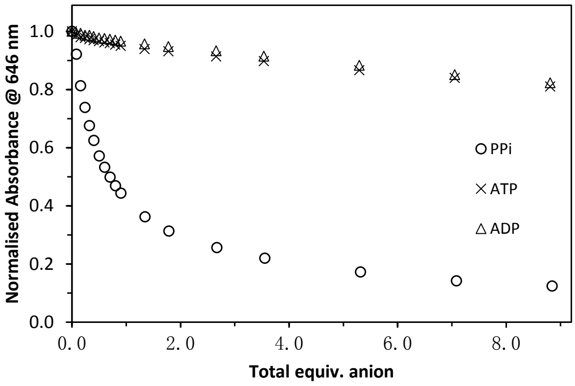

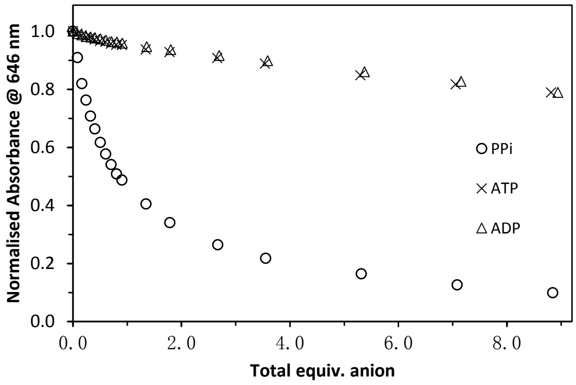

Figure S7: Normalised absorbance changes at 646 nm for the 1 : 1 mixture of (left) **1·Zn₂** : **PV** (20 μM) and (right) **2·Zn₂** : **PV** (20 μM) upon the addition of anions ($0-9$ equiv.).

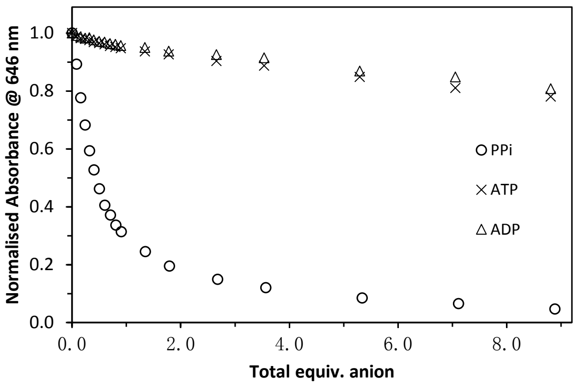

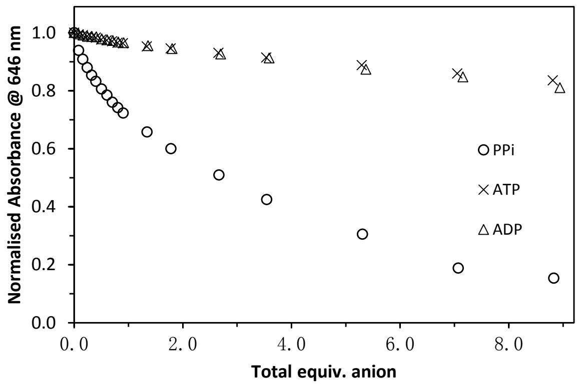

Figure S8: Normalised absorbance changes at 646 nm for the 1 : 1 mixture of (left) **3·Zn₂** : **PV** (20 μM) and (right) **4·Zn₂** : **PV** (20 μM) upon the addition of anions ($0-9$ equiv.).

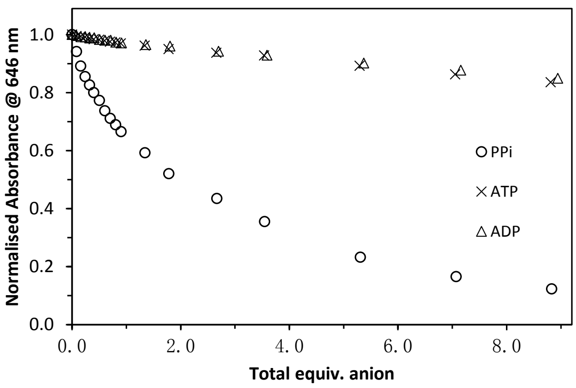

Figure S9: Normalised absorbance changes at 646 nm for the 1 : 1 mixture of **5·Zn₂** : **PV** (20 μM) upon the addition of anions ($0-9$ equiv.).

3.3 Speciation plots for receptor–PPi titrations

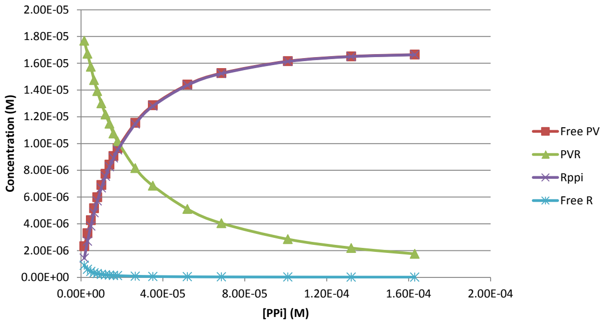

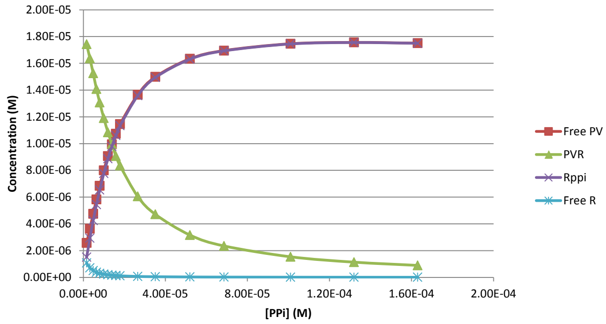

Figure S10: Speciation plot for the titration of (left) **1·Zn$_2$** : **PV** (20 µM) and (right) **2·Zn$_2$** : **PV** (20 µM) during the titration with PPi.

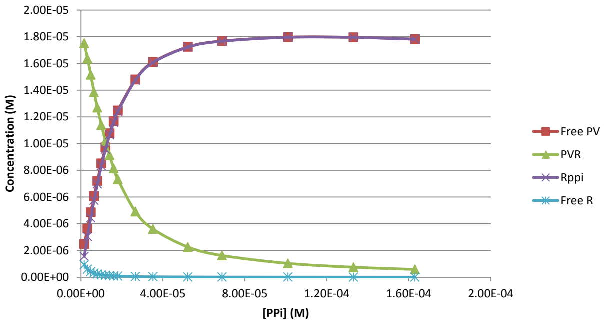

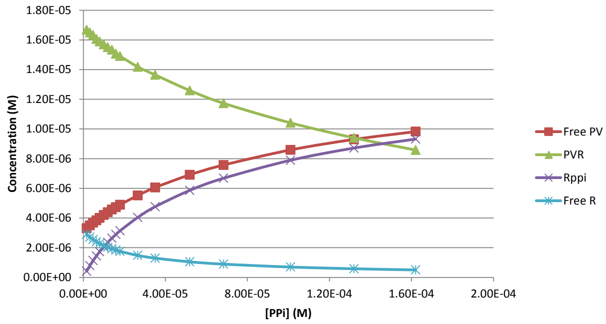

Figure S11: Speciation plot for the titration of (left) **3·Zn$_2$** : **PV** (20 µM) and (right) **4·Zn$_2$** : **PV** (20 µM) during the titration with PPi.

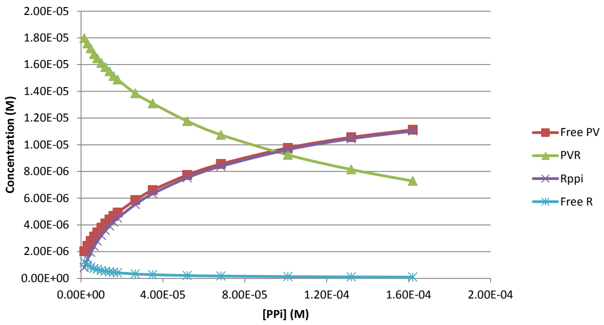

Figure S12: Speciation plot for the titration of (left) **3·Zn$_2$** : **PV** (20 µM) and (right) **4·Zn$_2$** : **PV** (20 µM) during the titration with PPi.

3.4 General procedure for Job's plot analysis

The overall concentration of the respective receptor and **PV** was adjusted to 40 µM and the absorbance spectra (250 – 750 nm) were recorded in Krebs buffer at 25 °C.

3.5 Job's plots for receptors 1–5·Zn_2 with PV

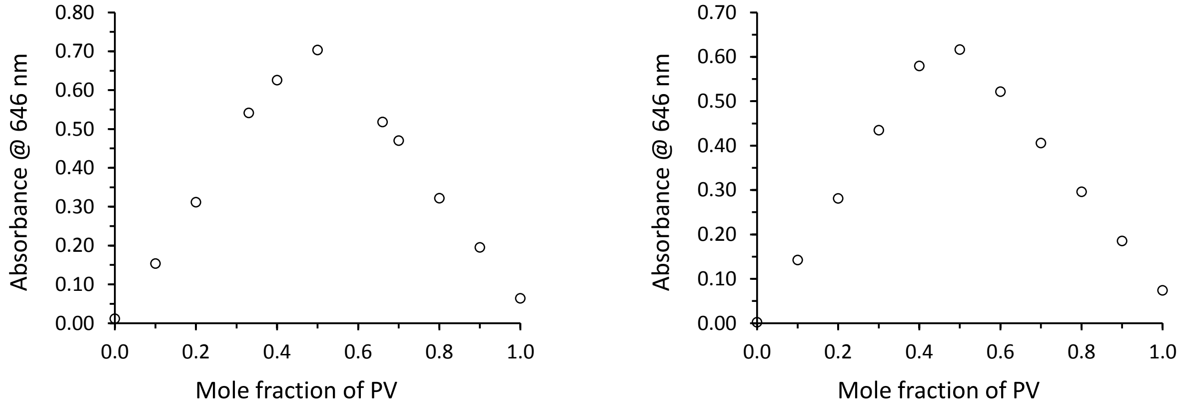

Figure S13: Job's plot for (left) **1·Zn_2** with **PV** and (right) **2·Zn_2** with **PV**.

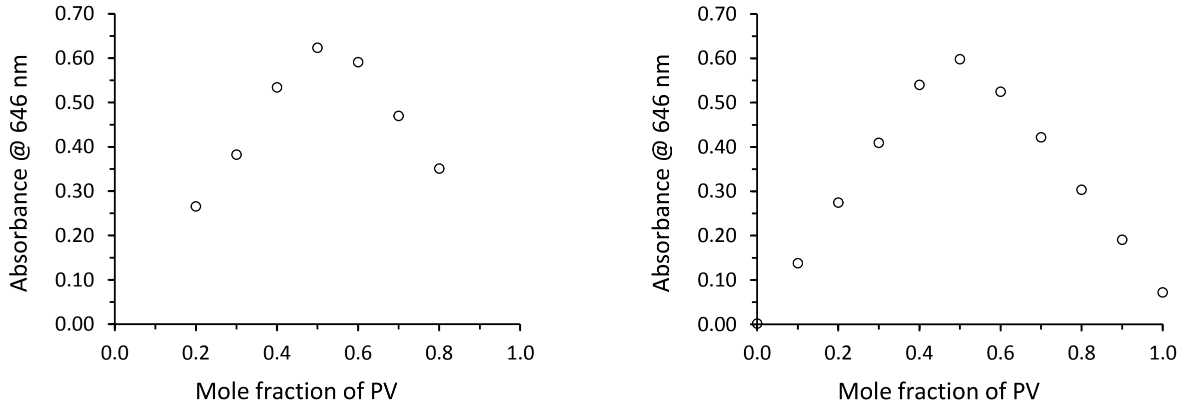

Figure S14: Job's plot for (left) **3·Zn_2** with **PV** and (right) **4·Zn_2** with **PV**.

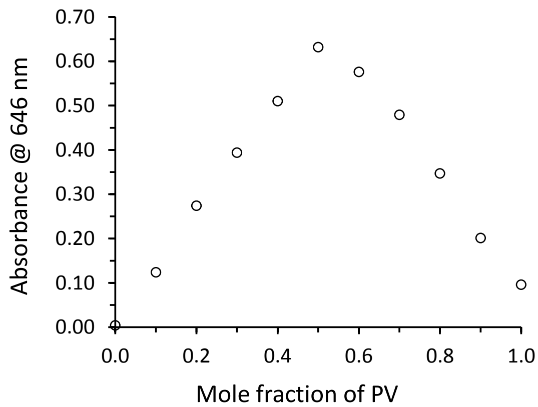

Figure S15: Job's plot for **5·Zn_2** with **PV**.

3.6 Molecular modelling

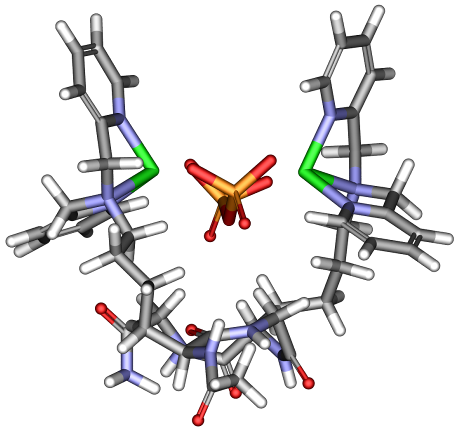

Figure S16: DFT-optimised molecular structure of the $\mathbf{3{\cdot}Zn_2}$–PPi complex.

3.7 1D and 2D NMR spectroscopic studies

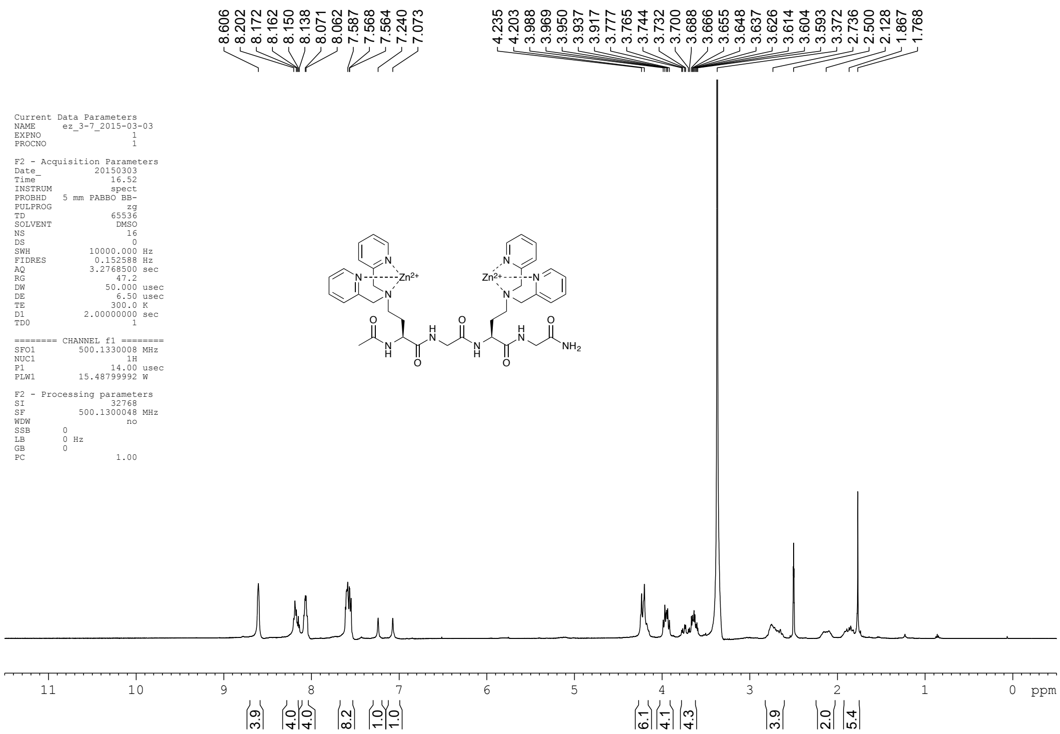

Figure S17: ^{1}H NMR spectrum (500 MHz) of Receptor $\mathbf{3{\cdot}Zn_2}$ in DMSO-d_6.

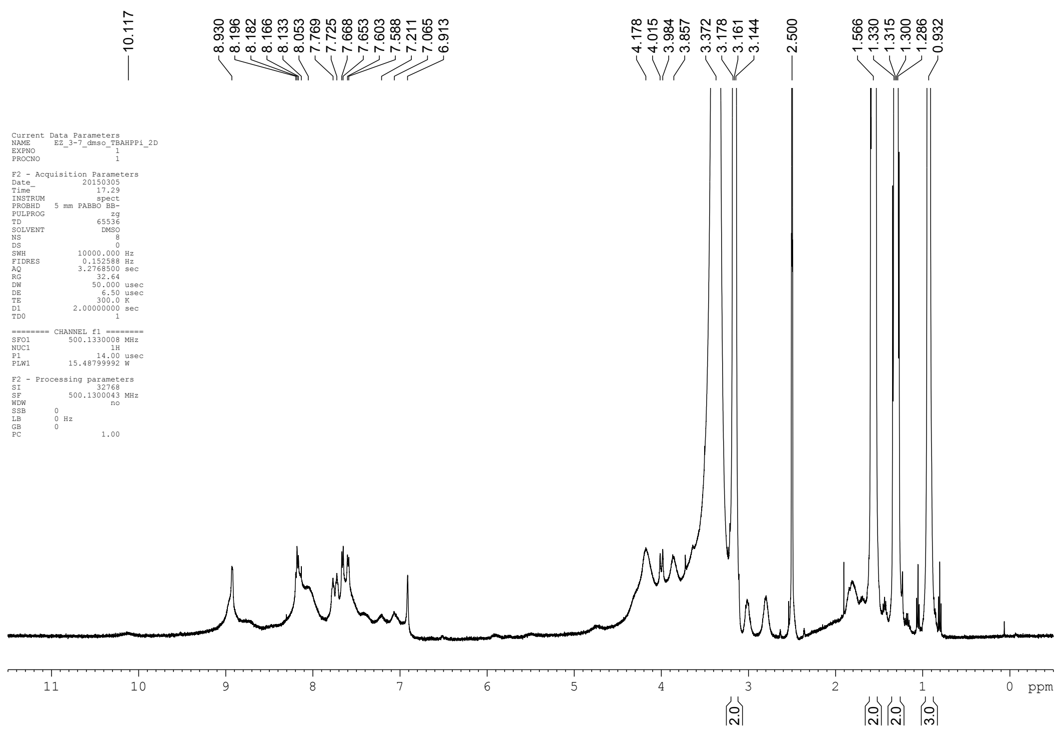

Figure S18: ^{1}H NMR spectrum (500 MHz) of Receptor $\mathbf{3{\cdot}Zn_2}$ in DMSO-d_6 with 1.0 equiv. HPPi.

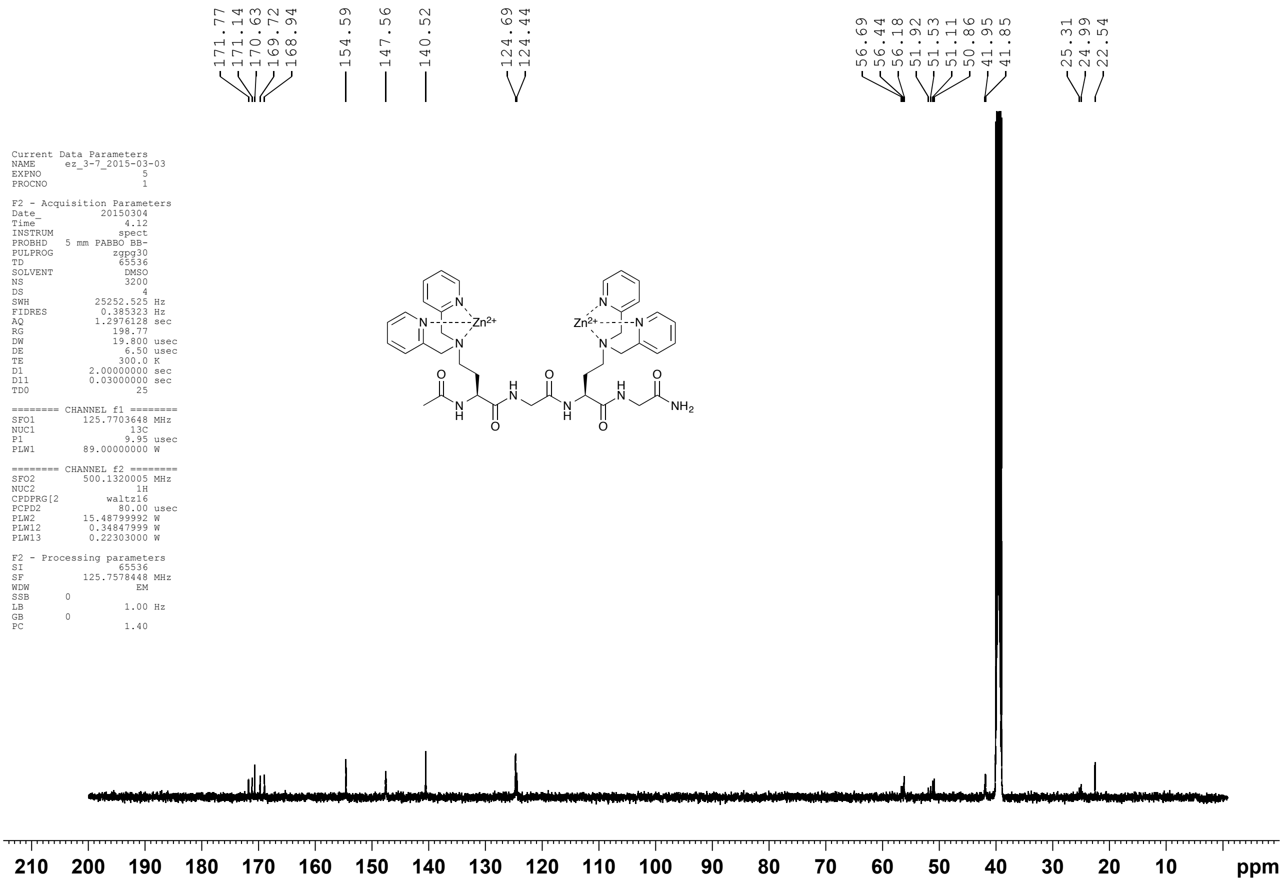

Figure S19: ^{13}C NMR spectrum (125 MHz) of receptor $\mathbf{3{\cdot}Zn_2}$ in DMSO-d_6.

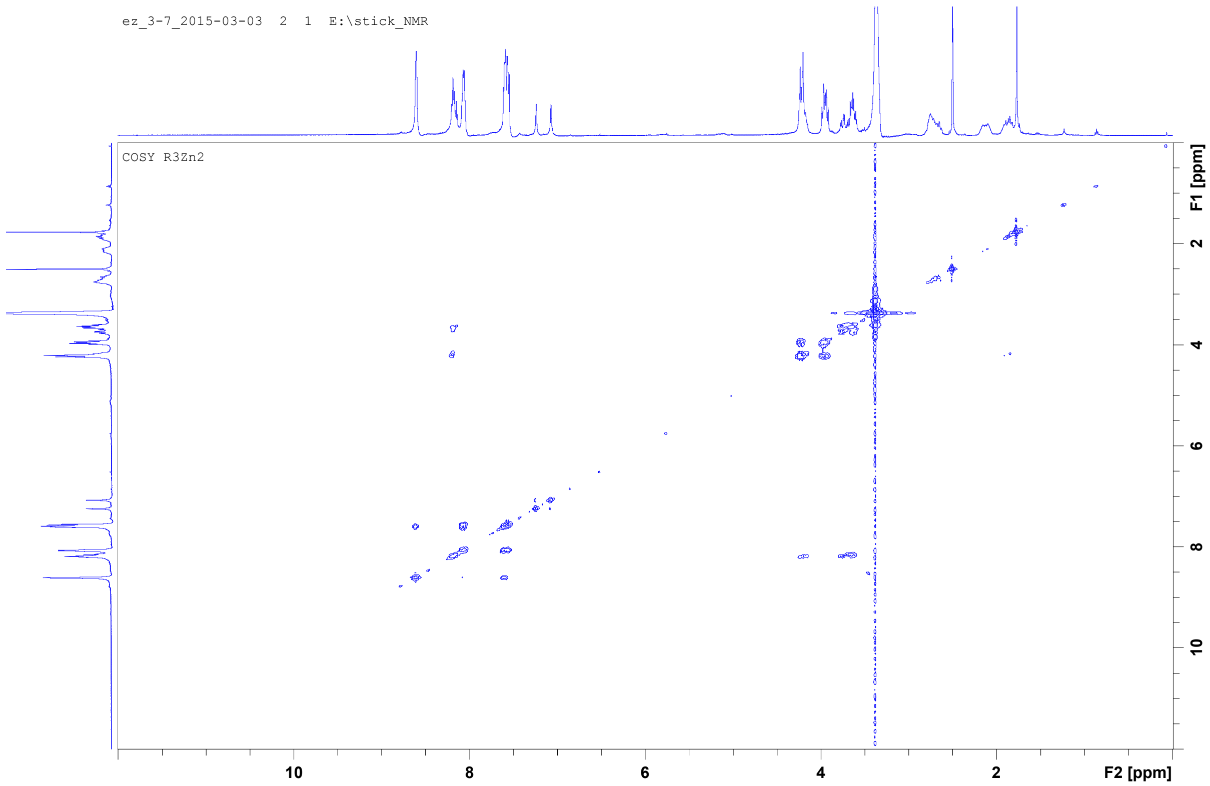

Figure S20: COSY spectrum (DMSO-d_6) of receptor $\mathbf{3{\cdot}Zn_2}$.

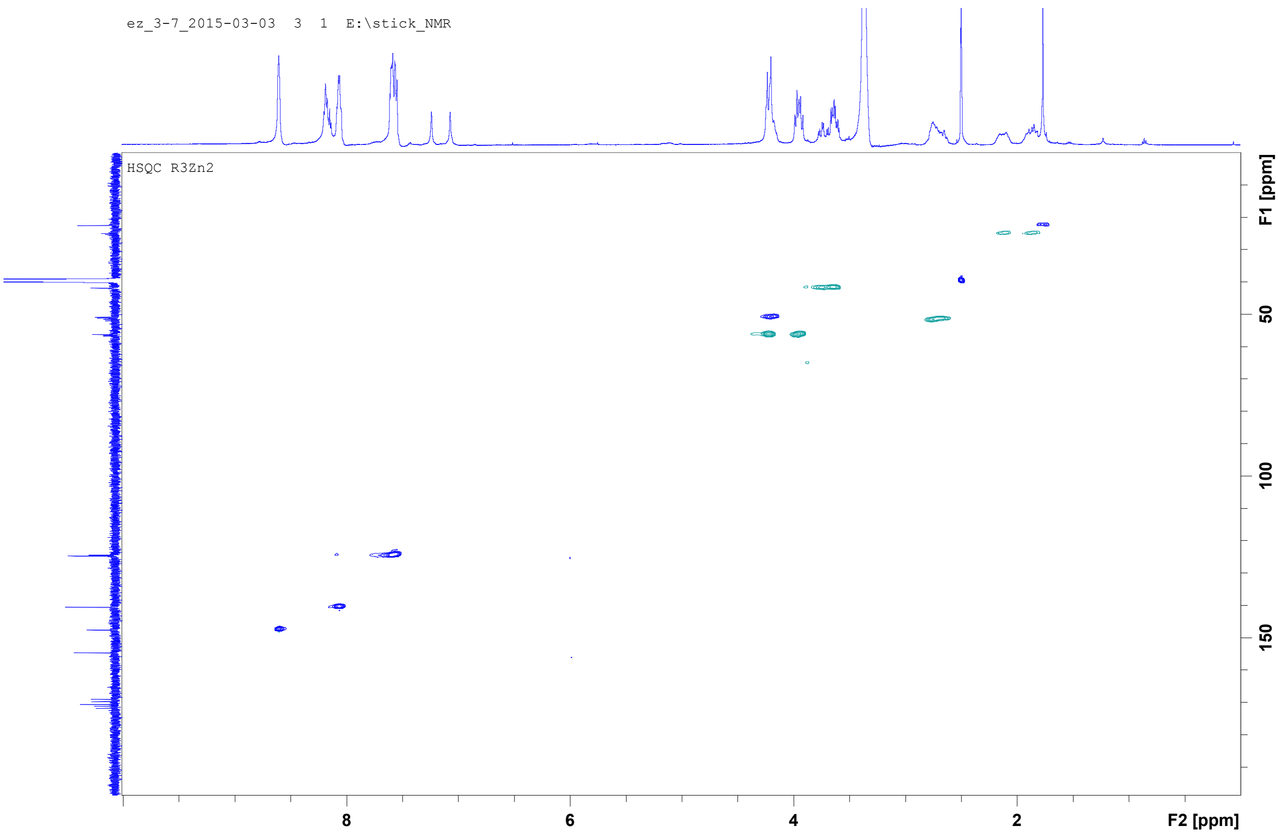

Figure S21: $^{1}H - ^{13}C$ HSQC spectrum (DMSO-d_6) of receptor $\mathbf{3{\cdot}Zn_2}$.

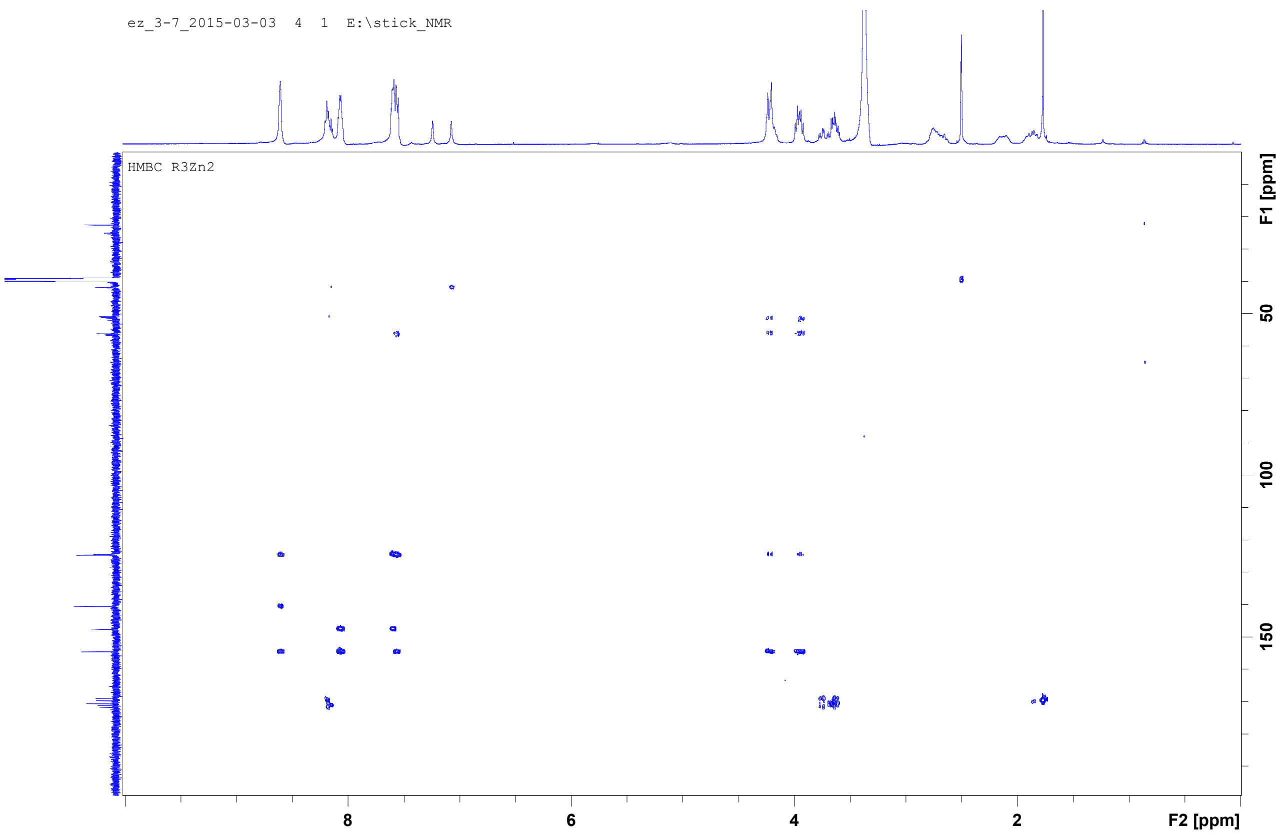

Figure S22: $^{1}H - ^{13}C$ HMBC spectrum (DMSO-d_6) of receptor $\mathbf{3{\cdot}Zn_2}$.

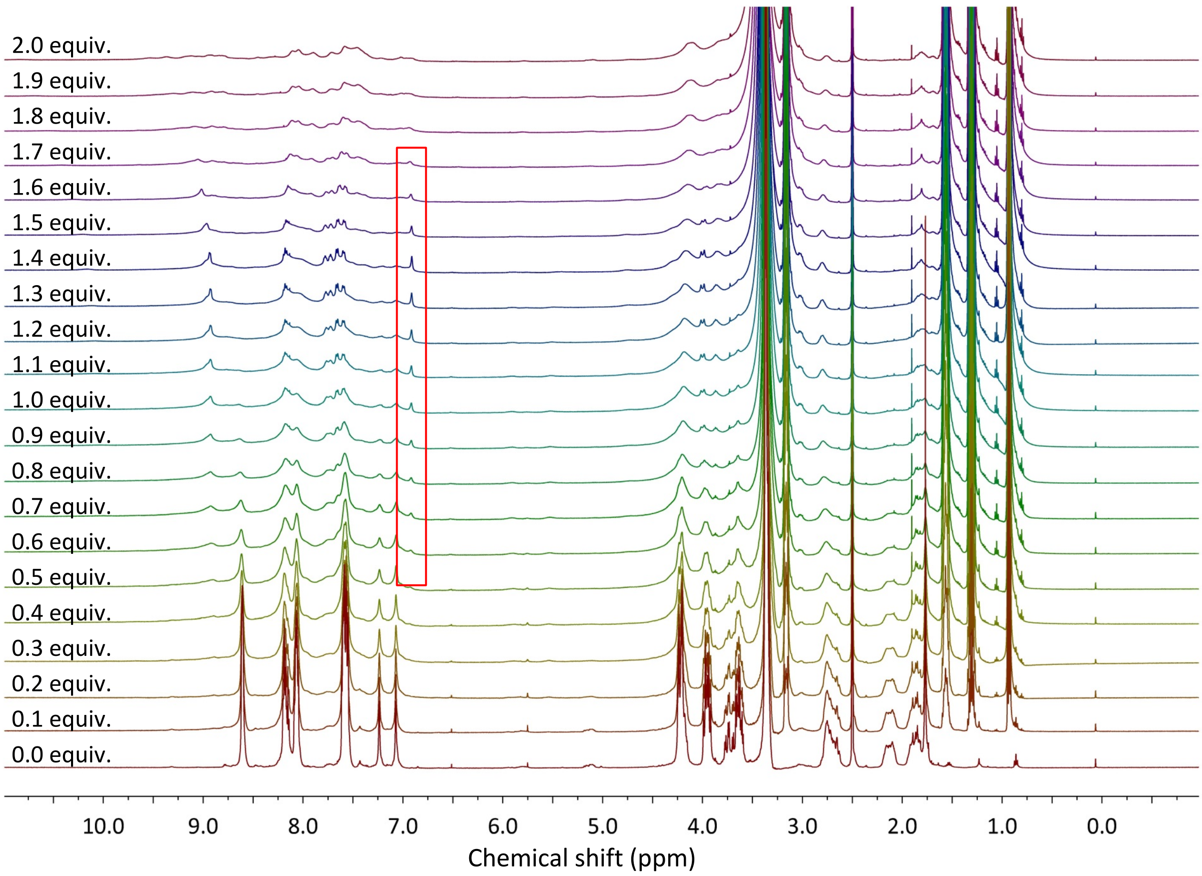

Figure S23: Stack plot of ^{1}H spectra of $\mathbf{3{\cdot}Zn_2}$ (20 mM) upon addition of HPPi as the TBA salt (0.0 − 2.0 equiv.) in DMSO at 300 K. The red rectangle highlights the emerging NH signal at 6.9 ppm.

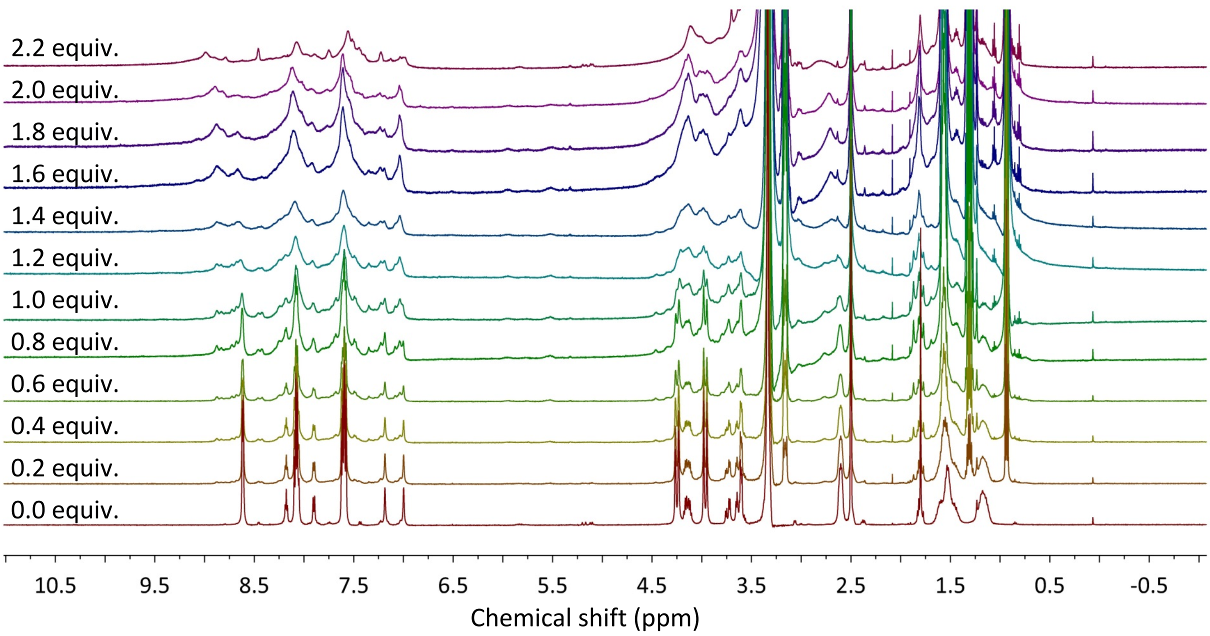

Figure S24: Stack plot of ^{1}H spectra of $\mathbf{1{\cdot}Zn_2}$ (20 mM) upon addition of HPPi as the TBA salt (0.0 − 2.2 equiv.) in DMSO at 300 K.

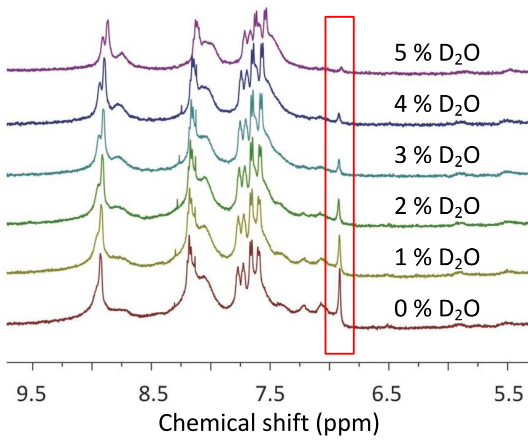

Figure S25: Stack plot of ^{1}H spectra of **3·Zn$_2$** (20 mM) containing 1.0 equiv. of HPPi as the TBA salt upon the addition of 0−5 vol% D_2O in DMSO at 300 K. The characteristic NH signal at 6.9 ppm decreases with an increasing amount of D_2O due to proton exchange.

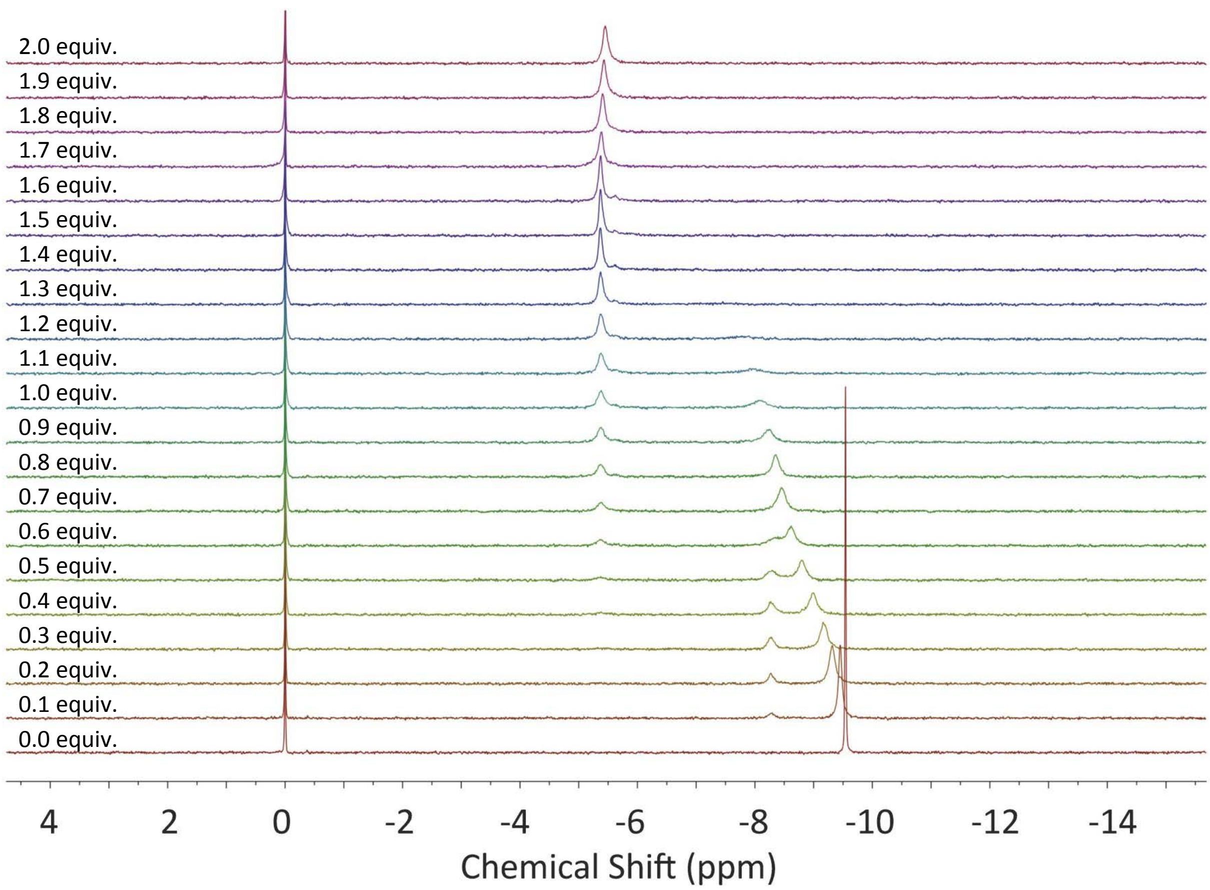

Figure S26: Stack plot of ^{31}P NMR spectra of PPi (20 mM) upon addition of **3·Zn$_2$** (0−2 equiv.) in D_2O at 300 K.

3.8 [PPi] calibration in Krebs buffer and artificial urine

All calibrations were repeated three times. Data analysis was performed according to a statistical treatment originally described by Hibbert and Gooding.[1]

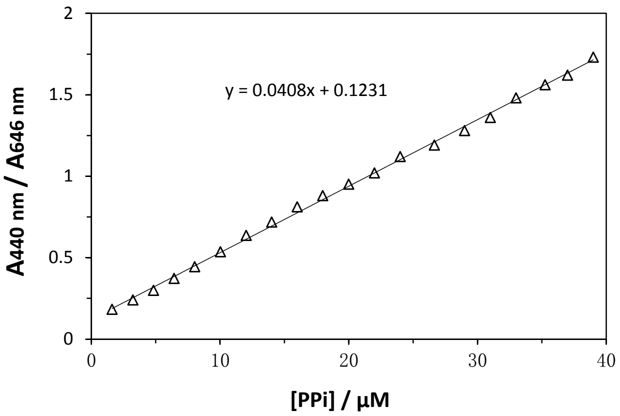

slope, b (µM^{-1})	0.040823128
standard deviation of slope, s_b (µM^{-1})	0.000368982
intercept a	0.123120298
standard deviation of intercept, s_a	0.008395703
standard error of regression, $s_{y/x}$	0.019209278
coefficient of determination, R^2	0.998531645
degrees of freedom, n-2	18
Fisher F statistic	12240.61560
explained variation	4.516742396
unexplained variation	0.006641934
detection limit (µM)	1.411646665

Figure S27: [PPi] calibration for **3·Zn$_2$** : **PV** (20 µM) in Krebs buffer.

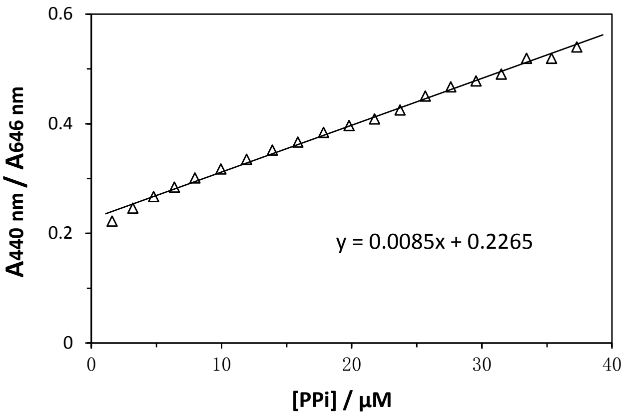

slope, b (µM^{-1})	0.008545781
standard deviation of slope, s_b (µM^{-1})	0.000141793
intercept a	0.226523444
standard deviation of intercept, s_a	0.003109516
standard error of regression, $s_{y/x}$	0.006992361
coefficient of determination, R^2	0.995069046
degrees of freedom, n-2	18
Fisher F statistic	3632.408935
explained variation	0.177599777
unexplained variation	0.000880076
detection limit (µM)	2.454671170

Figure S28: [PPi] calibration for **3·Zn$_2$** : **PV** (20 µM) in Krebs buffer and in the presence of 10 equiv. ATP.

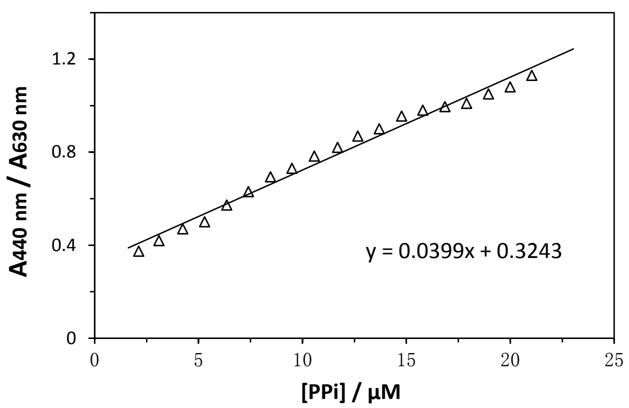

slope, b (µM^{-1})	0.039913390
standard deviation of slope, s_b (µM^{-1})	0.001268851
intercept a	0.324273360
standard deviation of intercept, s_a	0.016437894
standard error of regression, $s_{y/x}$	0.031866836
coefficient of determination, R^2	0.983109793
degrees of freedom, n-2	17
Fisher F statistic	989.5003963
explained variation	1.004832930
unexplained variation	0.017263419
detection limit (µM)	3.757516731

Figure S29: [PPi] calibration for **3·Zn$_2$** : **PV** (20 µM) in artificial urine.

3.9 Composition of Krebs buffer and of artificial urine

Table 1: Composition of Krebs buffer[a]

Component	M (g mol^{-1})	m (g L^{-1})	c (mM)
NaCl	58.4	8.01	137
KCl	74.6	0.40	5.4
$CaCl_2$	111.0	0.31	2.8
$MgSO_4.7H_2O$	246.5	0.30	1.2
KH_2PO_4	136.1	0.054	0.4
NaH_2PO_4	138.0	0.041	0.3
Glucose	180.2	1.80	10
TRIS	121.1	1.21	10

[a] The pH was adjusted to 7.4 with conc. HCl.

Table 2: Composition of artificial urine[2,b]

Component	M (g mol^{-1})	m (g L^{-1})	c (mM)
Peptone L37		1	
Yeast extract powder		0.01	
Lactic acid	90.1	0.10	1.1
Citric acid.H_2O	210.1	0.44	2.1
$NaHCO_3$	84.0	2.1	25
Urea	60.1	10	166
Uric acid[c]	168.1	0.035	0.2
Creatinine	113.1	0.80	7.1
$CaCl_2$ (dried)	111.0	0.28	2.5
NaCl	58.4	5.2	89
$FeSO_4.7H_2O$	278.0	0.0012	0.004
$MgSO_4.7H_2O$	246.5	0.49	2.0
Na_2SO_4 (anhydrous)	142.0	1.41	9.9
KH_2PO_4	136.1	0.95	7.0
K_2HPO_4	174.2	1.20	6.9
NH_4Cl	53.5	1.3	24

[b] The pH was adjusted to 7.4 with KOH.
[c] The original recipe suggests the addition of 0.07 g L^{-1} of uric acid; due to solubility issues we reduced the amount of uric acid to 0.035 g L^{-1}.

References

[1] Hibbert, D. B.; Gooding, J. J. *Data analysis for chemistry*; Oxford University Press, 2005.

[2] Brooks, T.; Keevil, C. *Lett. Appl. Microbiol.* **1997**, *24*, 203–206.